

UNCLASSIFIED

AFWAL-TR-80-3150

NL

1.44
2.25

END
DATE
FILMED
5-8h
DTIC

AD A097744

AFWAL-TR-80-3150

#2

AIR CUSHION LANDING SYSTEM STABILITY STUDY

DR. T. D. BURTON

*DEPARTMENT OF MECHANICAL ENGINEERING
WASHINGTON STATE UNIVERSITY
PULLMAN, WA 99164*

NOVEMBER 1980

AFWAL-TR-80-3150

Final Report for Period June 1980 — September 1980

Approved for public release; distribution unlimited.

DTIC FILE COPY

FLIGHT DYNAMICS LABORATORY
AIR FORCE WRIGHT AERONAUTICAL LABORATORIES
AIR FORCE SYSTEMS COMMAND
WRIGHT-PATTERSON AIR FORCE BASE, OHIO 45433


81 4 14 .27


NOTICE

When Government drawings, specifications, or other data are used for any purpose other than in connection with a definitely related Government procurement operation, the United States Government thereby incurs no responsibility nor any obligation whatsoever; and the fact that the government may have formulated, furnished, or in any way supplied the said drawings, specifications, or other data, is not to be regarded by implication or otherwise as in any manner licensing the holder or any other person or corporation, or conveying any rights or permission to manufacture, use, or sell any patented invention that may in any way be related thereto.

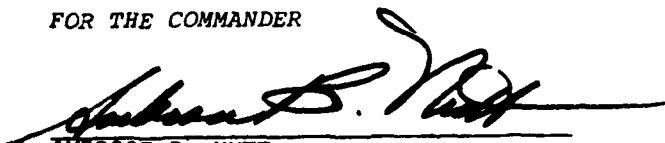
This report has been reviewed by the Information Office (OI) and is releasable to the National Technical Information Service (NTIS). At NTIS, it will be available to the general public, including foreign nations.

This technical report has been reviewed and is approved for publication.


DAVID L. FISCHER, 1Lt, USAF
Project Engineer
Special Projects Group
Mechanical Branch


AIVARS V. PETERSONS
Chief, Mechanical Branch
Vehicle Equipment Division

FOR THE COMMANDER


AMBROSE B. NUTT
Director, Vehicle Equipment Division
Flight Dynamics Laboratory

"If your address has changed, if you wish to be removed from our mailing list, or if the addressee is no longer employed by your organization please notify AFWAL/FIEMB, W-PAFB, OH 45433 to help us maintain a current mailing list".

Copies of this report should not be returned unless return is required by security considerations, contractual obligations, or notice on a specific document.
AIR FORCE/56780/31 March 1981 - 80

UNCLASSIFIED

SECURITY CLASSIFICATION OF THIS PAGE (When Data Entered)

14 REPORT DOCUMENTATION PAGE		READ INSTRUCTIONS BEFORE COMPLETING FORM
1. REPORT NUMBER	2. GOVT ACCESSION NO.	3. RECIPIENT'S CATALOG NUMBER
18 AFWAL TR-80-3150	AD-A097744	9
4. TITLE (and Subtitle)		5. FUNDING NUMBERS
6 AIR CUSHION LANDING SYSTEM STABILITY STUDY.		Final Technical Report, 30 Jun - 19 Sep 80
7. AUTHOR(s)		6. PERFORMING ORG. REPORT NUMBER
Thomas, D./Burton 1		
9. PERFORMING ORGANIZATION NAME AND ADDRESS		8. CONTRACT OR GRANT NUMBER(s)
Department of Mechanical Engineering Washington State University Pullman WA 99164		15 F33615-80-K-3409 N
10. PROGRAM ELEMENT, PROJECT, TASK AREA & WORK UNIT NUMBERS		12. REPORT DATE
2402129		Feb 1981
11. CONTROLLING OFFICE NAME AND ADDRESS		13. NUMBER OF PAGES
Flight Dynamics Laboratory (AFWAL/FIEM) AF Wright Aeronautical Laboratories (AFSC) Wright-Patterson Air Force Base Ohio 45433		63
14. MONITORING AGENCY NAME & ADDRESS (if different from Controlling Office)		15. SECURITY CLASS. (of this report)
		Unclassified
		15a. DECLASSIFICATION/DOWNGRADING SCHEDULE
16. DISTRIBUTION STATEMENT (of this Report)		
Approved for Public Release; Distribution Unlimited		
17. DISTRIBUTION STATEMENT (of the abstract entered in Block 20, if different from Report)		
18. SUPPLEMENTARY NOTES		
19. KEY WORDS (Continue on reverse side if necessary and identify by block number)		
EASY AIR CUSHION LANDING SYSTEMS DYNAMIC ANALYSIS AIR CUSHION STABILITY TRUNK MODEL		
20. ABSTRACT (Continue on reverse side if necessary and identify by block number)		
<p>An analysis of an inelastic ACLS plunge mode dynamic model is presented. The ACLS has unrestrained side elements and frozen end elements. The model exhibits unstable behavior at certain operating conditions for which the side elements are in contact with the ground. A linear analysis showed this instability to be due mainly to the altitude sensitivities of the cushion to atmosphere airflows and the attendant influence on the dynamic pressure forces on the vehicle. The model instability can be alleviated by isolating side and end elements so that they are all unrestrained and by simultaneously venting the air cushion directly.</p>		

DD FORM 1 JAN 73 1473

EDITION OF 1 NOV 65 IS OBSOLETE

UNCLASSIFIED

SECURITY CLASSIFICATION OF THIS PAGE (When Data Entered)

A

New 4/22/83

SECURITY CLASSIFICATION OF THIS PAGE(When Data Entered)

Block #20 (cont'd)

→ to atmosphere.

B

SECURITY CLASSIFICATION OF THIS PAGE(When Data Entered)

FOREWORD

This report describes work conducted by personnel of Washington State University, by and under the direction of Thomas D. Burton, Assistant Professor, under Grant #F 33615-80-K-3409.

The work reported herein was performed during the period 30 June 1980-19 September 1980 and represents a continuation of work supported by Boeing Company, during the period September 1979-February 1980.

The author wishes to thank J.R. Kilner, Advanced Airplane Branch, Boeing Military Airplane Company, for his assistance in providing much of the numerical data used in this work.

Application For	<input checked="checked" type="checkbox"/>
1. CLASS	<input type="checkbox"/>
2. 3	<input type="checkbox"/>
3. 4	<input type="checkbox"/>
4. 5	
5. 6	
6. 7	
7. 8	
8. 9	
9. 10	
10. 11	
11. 12	
12. 13	
13. 14	
14. 15	
15. 16	
16. 17	
17. 18	
18. 19	
19. 20	
20. 21	
21. 22	
22. 23	
23. 24	
24. 25	
25. 26	
26. 27	
27. 28	
28. 29	
29. 30	
30. 31	
31. 32	
32. 33	
33. 34	
34. 35	
35. 36	
36. 37	
37. 38	
38. 39	
39. 40	
40. 41	
41. 42	
42. 43	
43. 44	
44. 45	
45. 46	
46. 47	
47. 48	
48. 49	
49. 50	
50. 51	
51. 52	
52. 53	
53. 54	
54. 55	
55. 56	
56. 57	
57. 58	
58. 59	
59. 60	
60. 61	
61. 62	
62. 63	
63. 64	
64. 65	
65. 66	
66. 67	
67. 68	
68. 69	
69. 70	
70. 71	
71. 72	
72. 73	
73. 74	
74. 75	
75. 76	
76. 77	
77. 78	
78. 79	
79. 80	
80. 81	
81. 82	
82. 83	
83. 84	
84. 85	
85. 86	
86. 87	
87. 88	
88. 89	
89. 90	
90. 91	
91. 92	
92. 93	
93. 94	
94. 95	
95. 96	
96. 97	
97. 98	
98. 99	
99. 100	
100. 101	
101. 102	
102. 103	
103. 104	
104. 105	
105. 106	
106. 107	
107. 108	
108. 109	
109. 110	
110. 111	
111. 112	
112. 113	
113. 114	
114. 115	
115. 116	
116. 117	
117. 118	
118. 119	
119. 120	
120. 121	
121. 122	
122. 123	
123. 124	
124. 125	
125. 126	
126. 127	
127. 128	
128. 129	
129. 130	
130. 131	
131. 132	
132. 133	
133. 134	
134. 135	
135. 136	
136. 137	
137. 138	
138. 139	
139. 140	
140. 141	
141. 142	
142. 143	
143. 144	
144. 145	
145. 146	
146. 147	
147. 148	
148. 149	
149. 150	
150. 151	
151. 152	
152. 153	
153. 154	
154. 155	
155. 156	
156. 157	
157. 158	
158. 159	
159. 160	
160. 161	
161. 162	
162. 163	
163. 164	
164. 165	
165. 166	
166. 167	
167. 168	
168. 169	
169. 170	
170. 171	
171. 172	
172. 173	
173. 174	
174. 175	
175. 176	
176. 177	
177. 178	
178. 179	
179. 180	
180. 181	
181. 182	
182. 183	
183. 184	
184. 185	
185. 186	
186. 187	
187. 188	
188. 189	
189. 190	
190. 191	
191. 192	
192. 193	
193. 194	
194. 195	
195. 196	
196. 197	
197. 198	
198. 199	
199. 200	
200. 201	
201. 202	
202. 203	
203. 204	
204. 205	
205. 206	
206. 207	
207. 208	
208. 209	
209. 210	
210. 211	
211. 212	
212. 213	
213. 214	
214. 215	
215. 216	
216. 217	
217. 218	
218. 219	
219. 220	
220. 221	
221. 222	
222. 223	
223. 224	
224. 225	
225. 226	
226. 227	
227. 228	
228. 229	
229. 230	
230. 231	
231. 232	
232. 233	
233. 234	
234. 235	
235. 236	
236. 237	
237. 238	
238. 239	
239. 240	
240. 241	
241. 242	
242. 243	
243. 244	
244. 245	
245. 246	
246. 247	
247. 248	
248. 249	
249. 250	
250. 251	
251. 252	
252. 253	
253. 254	
254. 255	
255. 256	
256. 257	
257. 258	
258. 259	
259. 260	
260. 261	
261. 262	
262. 263	
263. 264	
264. 265	
265. 266	
266. 267	
267. 268	
268. 269	
269. 270	
270. 271	
271. 272	
272. 273	
273. 274	
274. 275	
275. 276	
276. 277	
277. 278	
278. 279	
279. 280	
280. 281	
281. 282	
282. 283	
283. 284	
284. 285	
285. 286	
286. 287	
287. 288	
288. 289	
289. 290	
290. 291	
291. 292	
292. 293	
293. 294	
294. 295	
295. 296	
296. 297	
297. 298	
298. 299	
299. 300	
300. 301	
301. 302	
302. 303	
303. 304	
304. 305	
305. 306	
306. 307	
307. 308	
308. 309	
309. 310	
310. 311	
311. 312	
312. 313	
313. 314	
314. 315	
315. 316	
316. 317	
317. 318	
318. 319	
319. 320	
320. 321	
321. 322	
322. 323	
323. 324	
324. 325	
325. 326	
326. 327	
327. 328	
328. 329	
329. 330	
330. 331	
331. 332	
332. 333	
333. 334	
334. 335	
335. 336	
336. 337	
337. 338	
338. 339	
339. 340	
340. 341	
341. 342	
342. 343	
343. 344	
344. 345	
345. 346	
346. 347	
347. 348	
348. 349	
349. 350	
350. 351	
351. 352	
352. 353	
353. 354	
354. 355	
355. 356	
356. 357	
357. 358	
358. 359	
359. 360	
360. 361	
361. 362	
362. 363	
363. 364	
364. 365	
365. 366	
366. 367	
367. 368	
368. 369	
369. 370	
370. 371	
371. 372	
372. 373	
373. 374	
374. 375	
375. 376	
376. 377	
377. 378	
378. 379	
379. 380	
380. 381	
381. 382	
382. 383	
383. 384	
384. 385	
385. 386	
386. 387	
387. 388	
388. 389	
389. 390	
390. 391	
391. 392	
392. 393	
393. 394	
394. 395	
395. 396	
396. 397	
397. 398	
398. 399	
399. 400	
400. 401	
401. 402	
402. 403	
403. 404	
404. 405	
405. 406	
406. 407	
407. 408	
408. 409	
409. 410	
410. 411	
411. 412	
412. 413	
413. 414	
414. 415	
415. 416	
416. 417	
417. 418	
418. 419	
419. 420	
420. 421	
421. 422	
422. 423	
423. 424	
424. 425	
425. 426	
426. 427	
427. 428	
428. 429	
429. 430	
430. 431	
431. 432	
432. 433	
433. 434	
434. 435	
435. 436	
436. 437	
437. 438	
438. 439	
439. 440	
440. 441	
441. 442	
442. 443	
443. 444	
444. 445	
445. 446	
446. 447	
447. 448	
448. 449	
449. 450	
450. 451	
451. 452	
452. 453	
453. 454	
454. 455	
455. 456	
456. 457	
457. 458	
458. 459	
459. 460	
460. 461	
461. 462	
462. 463	
463. 464	
464. 465	
465. 466	
466. 467	
467. 468	
468. 469	
469. 470	
470. 471	
471. 472	
472. 473	
473. 474	
474. 475	
475. 476	
476. 477	
477. 478	
478. 479	
479. 480	
480. 481	
481. 482	
482. 483	
483. 484	
484. 485	
485. 486	
486. 487	
487. 488	
488. 489	
489. 490	
490. 491	
491. 492	
492. 493	
493. 494	
494. 495	
495. 496	
496. 497	
497. 498	
498. 499	
499. 500	
500. 501	
501. 502	
502. 503	
503. 504	
504. 505	
505. 506	
506. 507	
507. 508	
508. 509	
509. 510	
510. 511	
511. 512	
512. 513	
513. 514	
514. 515	
515. 516	
516. 517	
517. 518	
518. 519	
519. 520	
520. 521	
521. 522	
522. 523	
523. 524	
524. 525	
525. 526	
526. 527	
527. 528	
528. 529	
529. 530	
530. 531	
531. 532	
532. 533	
533. 534	
534. 535	
535. 536	
536. 537	
537. 538	
538. 539	
539. 540	
540. 541	
541. 542	
542. 543	
543. 544	
544. 545	
545. 546	
546. 547	
547. 548	
548. 549	
549. 550	
550. 551	
551. 552	
552. 553	
553. 554	
554. 555	
555. 556	
556. 557	
557. 558	
558. 559	
559. 560	
560. 561	
561. 562	
562. 563	
563. 564	
564. 565	
565. 566	
566. 567	
567. 568	
568. 569	
569. 570	
570. 571	
571. 572	
572. 573	
573. 574	
574. 575	
575. 576	
576. 577	
577. 578	
578. 579	
579. 580	
580. 581	
581. 582	
582. 583	
583. 584	
584	

TABLE OF CONTENTS

SECTION		Page
I	INTRODUCTION	1
II	MODEL STABILITY BEHAVIOR	3
	1. System Model	3
	2. Techniques Used in Stability Analysis	9
	3. Analysis of Model Stability Behavior	17
III	MODEL VALIDITY ASSESSMENT	41
	1. Model Limit Cycle Behavior	41
	2. Trunk Model	47
	3. Effect of Pitch Motion	49
IV	CONCLUSIONS	51
V	RECOMMENDATIONS	52
	REFERENCES	53

LIST OF ILLUSTRATIONS

FIGURE	PAGE
1. System Model	2
2. Trunk Geometric Parameter Y_o , Z_{ofs} : Dependence on Pressure and Altitude Ratios	5
3. Trunk Geometric Parameters L_3 , A_s , A_{cv} : Dependence on Pressure and Altitude Ratios	6
4. Linear Stability Dependence on Trunk Flow W_{tr}	8
5. Pressure Phasing Relations Before and After Ground Contact	24
6. Effect of Damping Model on Plunge Mode Stability	30
7. Effect on Stability of Cushion End Flow W_{cu} /Altitude Sensitivity	35
8. Limit Cycle Behavior: $W_{tr} = 770$ lb/min, Nominal $W_{cu}/(h-h_{cu})$	42
9. Limit Cycle Behavior: $W_{tr} = 770$ lb/min, $W_{cu}/(h-h_{cu}) = .2$ of Nominal	43
10. Limit Cycle Behavior: $W_{tr} = 840$ lb/min, Nominal $W_{cu}/(h-h_{cu})$	45
11. Limit Cycle Behavior: $W_{tr} = 840$ lb/min, $W_{cu}/(h-h_{cu}) = .25$ of Nominal	46

LIST OF TABLES

TABLE		PAGE
1.	Linearized Variation Equations	12
2.	Stability Technique Verification	13
3.	Linearized Variation Equations for Reduced Operating Pressure Ratio	33

LIST OF SYMBOLS

A_s, A_{cv}	= trunk cross section area, fraction of trunk cross section area, respectively (Figure 1) $\sim \text{in}^2$
C, S	= cosine and sine coefficients of output cushion pressure, equation (20)
CA	= flow coefficient $\sim \text{in}^2$
D	= trunk section length $\sim \text{in}$
D_{MP}	= coefficient of damping due to trunk/ground contact $\sim \text{lb-sec/ft}$
g	= gravitational acceleration $\sim \text{ft/sec}^2$
h	= vehicle altitude (c.g.) $\sim \text{ft}$
h_{cu}	= distance from c.g. to bottom of rigid trunk end element $\sim \text{in}$
k_{RT}	= constant in pressure equations
K_c, K_s	= cosine and sine coefficients of input to pressure system, equation (19)
L	= lift $\sim \text{lb}$
L_3	= width of trunk-ground contact region (Figure 1) $\sim \text{in}$
M	= vehicle mass $\sim \text{slugs}$
p_a, p_c, p_t	= ambient, cushion and trunk pressures, respectively $\sim \text{psi}$
P_r	= pressure ratio $\equiv (p_c - p_a)/(p_t - p_a)$
T, Δ	= trace and determinant of pressure system submatrix $[P]$, respectively.
V_c, V_t	= cushion, trunk volumes $\sim \text{in}^3$
w	= vehicle velocity, positive downward $\sim \text{ft/sec}$
W	= air flow rate $\sim \text{lbm/sec}$
Y_a	= distance from trunk inboard attachment to vehicle geometric center (Figure 1) $\sim \text{in}$
Y_o	= horizontal distance from trunk inboard attachment to lowest point on trunk (Figure 1) $\sim \text{in}$

LIST OF SYMBOLS (concluded)

Z_{gap}	= gap between trunk bottom and ground ~ in
Z_o	= distance, vehicle bottom to trunk bottom (Figure 1) ~ in
Z_{ofs}	= Z_o which would exist if there were no ground contact ~ in
Z_r	= Z_o/Z_{ofs} (prior to ground contact $Z_r = 1$)
$\delta ()$	= small change in ()
γ	= ratio of specific heat = 1.4
λ	= stability matrix eigenvalues
ϕ_I, ϕ_o, ϕ_T	= input, output, and total phase shifts of pressure system
σ, ω	= real and imaginary parts, respectively, of plunge mode eigenvalue.

Subscripts

ca	= cushion to atmosphere
tc	= trunk to cushion
ta	= trunk to atmosphere
cu	= cushion end to atmosphere
tr	= trunk

Matrices

$[A], a_{ij}$	= stability matrix, element of stability matrix (4 x 4)
$[P]$	= "pressure system" submatrix = $\begin{bmatrix} a_{11} & a_{12} \\ a_{21} & a_{22} \end{bmatrix}$
$[P_h]$	= "pressure/altitude" submatrix = $\begin{bmatrix} a_{13} & a_{14} \\ a_{23} & a_{24} \end{bmatrix}$
$[H_p]$	= "altitude/pressure" submatrix = $\begin{bmatrix} a_{31} & a_{32} \\ a_{41} & a_{42} \end{bmatrix}$
$[H]$	= "altitude" submatrix = $\begin{bmatrix} a_{33} & a_{34} \\ a_{43} & a_{44} \end{bmatrix}$

SUMMARY

A combined vehicle/air cushion landing system dynamic model recently developed by Boeing Company exhibits unstable behavior for certain operating conditions. The objectives of this study were 1) to ascertain the reason for this instability and to isolate the important physical effects involved, 2) to suggest means to alleviate the instability, and 3) to assess the validity of the model and results obtained. The model considered consisted of a vehicle constrained to move vertically and supported by an inelastic trunk whose side elements were unrestrained and whose end elements were frozen.

The stability was investigated by linearizing the model state equations. This was done by simplifying the model such that the vertical motion and the pressure responses were considered to be those of quasi-coupled mechanical oscillators. Use of this approach enabled the stability behavior to be described in such a way that the influence of each system parameter could be seen.

For the model studied, instability occurred when operating conditions were such that the side trunk elements first contacted the ground. This contact shuts off the air flow under the side elements, while still allowing flow under the frozen end elements. This flow combination substantially alters the system pressure response, which in turn causes a destabilization of the vertical motion. The instability could be eliminated by arranging the trunk so that the side and end elements contact the ground simultaneously and then by venting the air cushion directly to atmosphere through a constant area orifice.

Stability calculations were also made for a trunk with all elements frozen, and for this model the stability behavior was quite different than for the unrestrained model. This result illustrated that the stability is sensitive to

trunk geometry changes which accompany changes in pressure and altitude. It appears that the best stability behavior can be achieved by allowing both side and end elements to be as unrestrained as possible (this could be accomplished, for example, with a bellows arrangement at each "corner" of the trunk) and by simultaneously venting the cushion directly to atmosphere.

Results obtained for the trunk model considered appear physically reasonable. The response is similar to that exhibited by self-excited oscillators; the energy source here appears to be the power needed to provide the input trunk flow. In comparing the model analyzed to an actual trunk, we note that the restraining influence of the trunk curvature (in the horizontal plane) which would exist at the "corners" of a single piece trunk has not been taken into account here. For a trunk whose side elements are substantially longer than the end elements, the model analyzed in this study should be adequate, but test verification of this conclusion would be desirable.

A useful result is that the analysis approach employed provides a systematic technique with which a given trunk/vehicle system may be designed so as to provide acceptable stability.

SECTION I

INTRODUCTION

Presented is an analysis of the stability characteristics of the Air Cushion Landing System dynamic model developed by Boeing Co. (Ref. 1). The combined vehicle/ACLS model exhibits an unstable oscillatory motion for certain operating conditions. The objectives of the work were to determine which model parameters are most important in governing vehicle stability, to provide a physical interpretation of these effects, and hence to assess the physical believability of such effects. Potential means of alleviating the instability were also addressed. The work represents a continuation of an analysis supported by Boeing Company and conducted during November - January 1979-80 (Ref. 2).

The system considered was a plunge mode model with vehicle and trunk parameters representative of the Jindivik aircraft (Figure 1). Although this model is considerably simplified relative to the complete six degree of freedom ACLS model described in Reference 1, it does exhibit similar stability characteristics. Thus, an understanding of the behavior of this simple system should enable the important effects on stability to be uncovered. In order to make the present report as self contained as possible, some of the work reported in Reference 2 is included herein.

In the following sections are presented the system model equations, the linear stability analysis techniques (and their verification), interpretation of the model stability behavior, and some parametric results which indicate means of alleviating the instability.

A primary objective of the work was the development of stability analysis methods which would display directly the influence of the various system parameters on stability. Although this was accomplished, the resulting mathematical description is complicated due to the large number of individual parameters involved. Thus, to properly explain model stability behavior, a detailed discussion of the stability relations has been necessary.

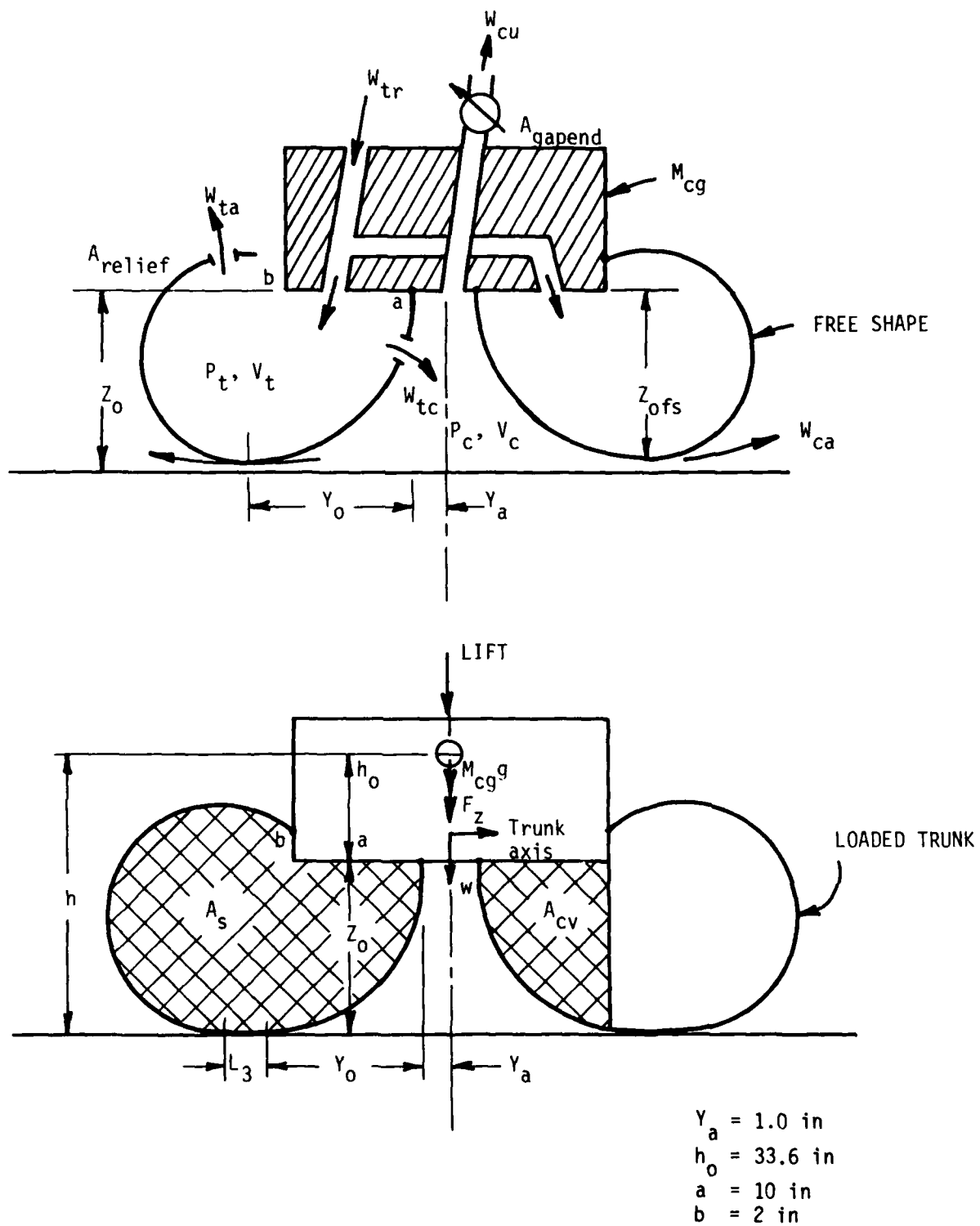


Figure 1 - System Model

SECTION II

MODEL STABILITY BEHAVIOR

1. System Model

The plunge mode model considered is shown in Figure 1. The dynamics are described by four states: trunk and cushion pressures P_t and P_c , and altitude h and vertical velocity $w = -\dot{h}$ (w is measured positive downward). The system equations of motion are given below and represent a simplification of the Boeing model described in Ref. 1:

$$\dot{P}_t = \frac{kRT}{V_t} (W_{tr} - W_{tc} - W_{ta}) - kP_t \dot{V}_t/V_t \quad (1)$$

$$\dot{P}_c = \frac{kRT}{V_c} (-W_{cu} + W_{tc} - W_{ca}) - kP_c \dot{V}_c/V_c \quad (2)$$

$$\dot{w} = \frac{-2D}{M} \{L_3 (P_t - P_a + wD_{MP}) + (Y_a - Y_o)(P_c - P_a)\} + g + \frac{L}{M} \quad (3)$$

$$\dot{h} = -w \quad (4)$$

$$\dot{V}_t = 2DA_s \quad (5)$$

$$\dot{V}_c = 2D[Z_o(Y_a + Y_o) - A_{cv}] \quad (6)$$

where D is the length of the single trunk element on each side of the vehicle. The motion, as governed by these equations, is heavily dependent on the trunk geometric parameters which are shown in Figure 1. These are:

L_3 = width of trunk in contact with ground (in.)

Y_o = horizontal distance from inner trunk attachment to ground contact point, or if not in ground contact, to the horizontal tangency point (in.)

A_s = trunk cross-sectional area (in.²)

A_{cv} = fraction of A_s used in cushion volume calculation (in.²)

Z_o = distance from bottom of vehicle to ground (in.)

Z_{ofs} = distance from vehicle bottom to trunk bottom when trunk not in ground contact (in.)

These geometric parameters are functions of the pressure ratio $P_r \equiv (P_c - P_a)/(P_t - P_a)$, with P_a the ambient pressure, and the altitude ratio $Z_r = Z_o/Z_{ofs}$, where $Z_o = h - h_o$ and $Z_{ofs} = Z_{ofs}(P_r)$. The dependence of these geometric parameters on pressure and altitude ratios P_r and Z_r is shown in Figures 2 and 3 for the inelastic trunk model considered here. These dependencies will be shown to have an important effect on the vehicle motion.

The various air flows which govern cushion and trunk pressure change are calculated using the compressible flow relations given below:

$$W_{ca} = CA_{ca} P_c \left\{ \frac{2g}{RT} \frac{\gamma}{\gamma-1} \left[\left(\frac{P_a}{P_c} \right)^{2/\gamma} - \left(\frac{P_a}{P_c} \right)^{\frac{\gamma+1}{\gamma}} \right] \right\}^{1/2} \quad (7)$$

$$W_{tc} = CA_{tc} P_t \left\{ \frac{2g}{RT} \frac{\gamma}{\gamma-1} \left[\left(\frac{P_c}{P_t} \right)^{2/\gamma} - \left(\frac{P_c}{P_t} \right)^{\frac{\gamma+1}{\gamma}} \right] \right\}^{1/2} \quad (8)$$

$$W_{ta} = CA_{ta} P_t \left\{ \frac{2g}{RT} \frac{\gamma}{\gamma-1} \left[\left(\frac{P_a}{P_t} \right)^{2/\gamma} - \left(\frac{P_a}{P_t} \right)^{\frac{\gamma+1}{\gamma}} \right] \right\}^{1/2} \quad (9)$$

$$W_{cu} = CA_{cu} P_c \left\{ \frac{2g}{RT} \frac{\gamma}{\gamma-1} \left[\left(\frac{P_a}{P_c} \right)^{2/\gamma} - \left(\frac{P_a}{P_c} \right)^{\frac{\gamma+1}{\gamma}} \right] \right\}^{1/2} \quad (10)$$

where, for the system under consideration, the area flow coefficients are given by:

$$CA_{ca} = 1.8 D Z_{gap} \quad (\text{in.}^2)$$

$$CA_{tc} = 18.163$$

$$CA_{ta} = 17.73$$

$$CA_{cu} = 90.72 (12 h - h_{cu})$$

where $Z_{gap} = 0$ when the trunk contacts the ground and $Z_{gap} = Z_o - Z_{ofs}$ otherwise.

The cushion to atmosphere end flow (i.e., out of the paper, Figure 1), W_{cu} , is defined in terms of the altitude h_{cu} , which is the distance from the vehicle c.g. to the bottom of the end trunk sections. These end trunk sections are assumed to be

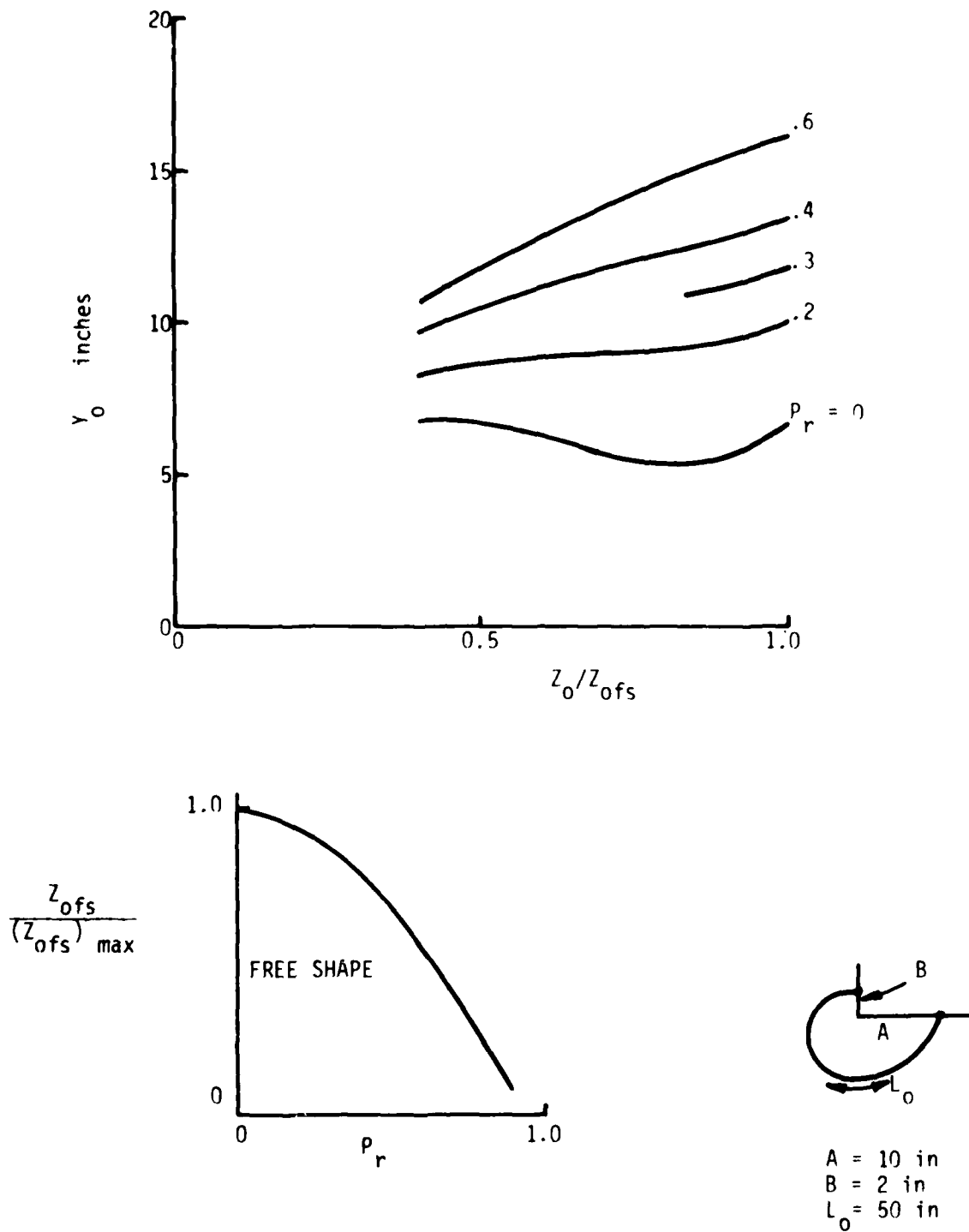


Figure 2 - Trunk Geometric Parameter Y_0 , Z_{0fs} : Dependence on Pressure and Altitude Ratios

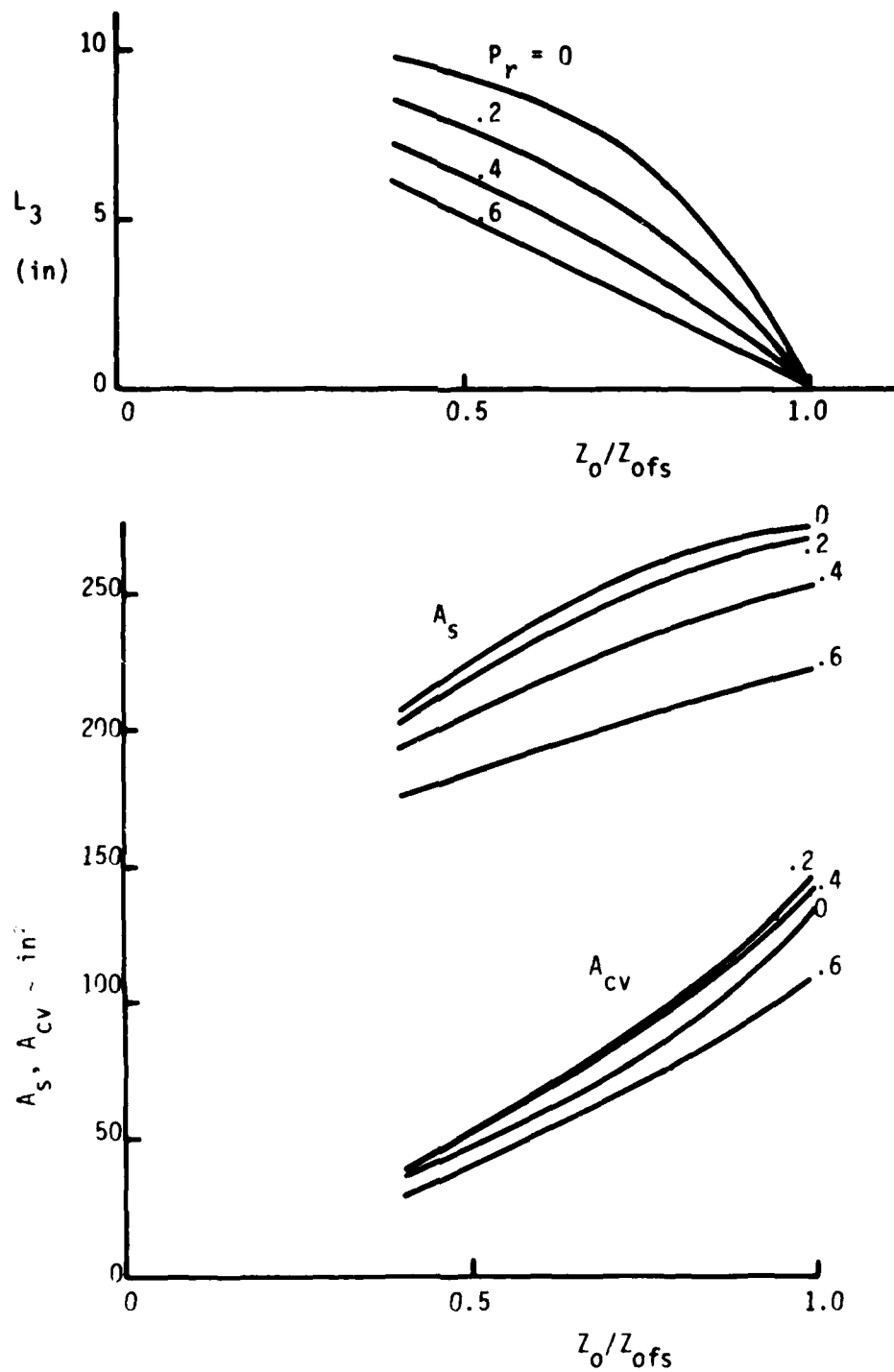


Figure 3 - Trunk Geometric Parameters L_3 , A_s , A_{cv} : Dependence on Pressure and Altitude Ratios

frozen. Note that the trunk to cushion and trunk to atmosphere flows W_{tc} and W_{ta} depend only on the associated pressure differences, whereas the cushion to atmosphere and cushion end flows W_{ca} and W_{cu} depend in addition on the altitude. It will be seen later that these flow/altitude sensitivities dominate the vehicle stability. All of the flows are defined by equations (7-10) to be positive. The signs (negative indicating flow out of) are taken into account in the system equations. The system equilibrium, or operating point, is defined by equations (1)-(4) with all derivatives zero,

$$\begin{aligned} W_{tr} - W_{tc} - W_{ta} &= 0 \\ -W_{cu} + W_{tc} - W_{ca} &= 0 \\ \frac{2D}{M} [L_3(P_t - P_a) + (Y_a - Y_o)(P_c - P_a)] &= g + \frac{L}{M} \end{aligned}$$

Due to the nature of the flow relations and the trunk geometric parameters, the system is highly nonlinear and difficult to analyze analytically. The stability of small motions about equilibrium was assessed by Boeing by numerically calculating the Jacobian matrix and associated eigenvalues. For the present system the plunge mode eigenvalue variation with trunk flow rate W_{tr} is shown in Figure 4. The flow rate $W_{tr} \cong 758$ lb/min corresponds to the initial contact of the trunk with the ground, which is accompanied by a gross instability. As the trunk flow is increased, accompanied by a larger portion of the trunk being in ground contact, the motion is less unstable until at $W_{tr} \cong 900$ lb/min stability once again ensues. The exact cause of this behavior could not be easily found from the numerical stability results since the influence of each of the many parameters involved was difficult to isolate.

In the following section, two analytical techniques used to assess this behavior are described and verified, i.e., demonstrated to yield the same stability information as calculated numerically and shown in Figure 4. Then, these techniques are used to explain the reason for the observed model behavior.

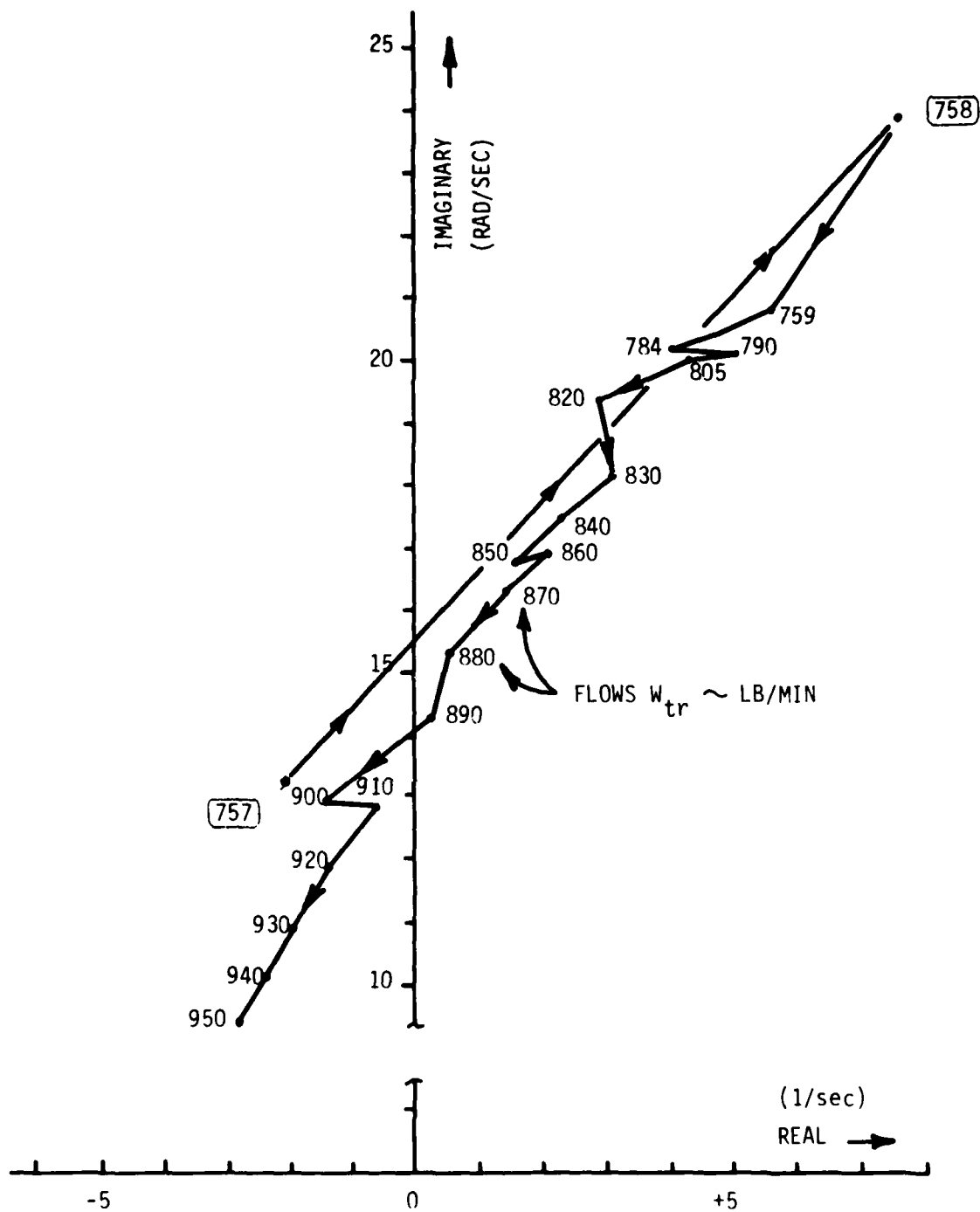


Figure 4 - Linear Stability Dependence on Trunk Flow W_{tr}

2. Techniques Used in Stability Analysis

a. System stability matrix

In order to see clearly the effect of individual parameters on the system stability matrix, the elements of the system matrix were determined analytically as described here. First, each of the four states (denoted for simplicity as x_i , $i = 1$ to 4) was assumed to be comprised of its equilibrium value x_{i0} plus some small deviation δx_i from equilibrium,

$$x_i = x_{i0} + \delta x_i \quad i = 1 \text{ to } 4. \quad (11)$$

These variational forms were substituted into the system equations (1) - (4) and the results were linearized to yield four linear first-order differential equations for the δx_i , of the form

$$\{\delta \dot{x}_i\} = [A] \{\delta x_i\} \quad (12)$$

where $[A]$ is the 4 x 4 Jacobian matrix. This procedure was algebraically complicated by two things: first, the flow relations given by equations (7) - (10) are unwieldy, so the variational procedure was applied to a simplified form of these relations obtained using the leading terms in the flow relations. This simplified model is summarized below:

$$W_{ca} \approx 1.8 D Z_{gap} (.04826) P_c \left(\frac{\Delta P_c}{P_a} \right)^{1/2} \text{ lb/sec}$$

$$W_{tc} \approx .8765 P_t \left(\frac{\Delta P_t - \Delta P_c}{P_a} \right)^{1/2} \text{ lb/sec}$$

$$W_{ta} \approx .8556 P_t \left(\frac{\Delta P_t}{P_a} \right)^{1/2} \text{ lb/sec}$$

$$W_{cu} \approx 90.7 (12h - h_{cu}) (.04826) P_c \left(\frac{\Delta P_c}{P_a} \right)^{1/2} \text{ lb/sec}$$

where $\Delta P_t \equiv P_t - P_a$ and $\Delta P_c \equiv P_c - P_a$.

These relations are generally accurate to within 10 or 15% when compared to equations (7) - (10). In the final Jacobian matrix, the flow rate variations are expressed as fractions of the actual equilibrium flow rates as calculated using the complete flow relations, so the above inaccuracy is not significant.

A second source of algebraic complexity lay in the dependence of the geometric parameters Y_o , L_3 , A_s , A_{cv} , etc. on the states P_c , P_t , and h . The variations in these parameters which accompany variations in the states P_t , P_c , and h were calculated using the chain rule to write everything in terms of the primary dependent variables,

$$\delta () = \frac{\partial ()}{\partial P_c} \delta P_c + \frac{\partial ()}{\partial P_t} \delta P_t + \frac{\partial ()}{\partial h} \delta h \quad (13)$$

where () stands for any of Y_o , L_3 , A_s , A_{cv} , V_c , V_t , or Z_{ofs} . Since the trunk geometry information is given in terms of P_r and Z_r , rather than in terms of P_c , P_t , and h explicitly, the individual partial derivatives appearing in equation (13) were calculated in terms of partial derivatives with respect to P_r and Z_r from

$$\begin{aligned} \frac{\partial}{\partial P_c} &= \frac{1}{\Delta P_{to}} \left\{ \frac{\partial}{\partial P_r} - \left(\frac{Z_r}{Z_{ofs}} \frac{\partial Z_{ofs}}{\partial P_r} \right) \frac{\partial}{\partial Z_r} \right\} \\ \frac{\partial}{\partial P_t} &= -P_r \frac{\partial}{\partial P_c} \\ \frac{\partial}{\partial h} &= \frac{12}{Z_{ofs}} \frac{\partial}{\partial Z_r} \end{aligned} \quad (14)$$

The twelve is included in the last of these because Z_{ofs} has units of inches, while h is in feet. In a fashion similar to the above, the variations in volume rates of change were obtained from, for example,

$$\delta \dot{V}_t = \frac{\partial V_t}{\partial P_t} \delta \dot{P}_t + \frac{\partial V_t}{\partial P_c} \delta \dot{P}_c - \frac{\partial V_t}{\partial h} \dot{w} \quad (15)$$

Note that the nature of equation (15) and the associated relation for $\delta \dot{V}_c$ means that the volume derivative effects are really proportional to $\delta \dot{P}_t$ and $\delta \dot{P}_c$; thus,

the variational forms of the pressure equations (1) and (2) will actually end up being simultaneous equations in $\delta\dot{P}_t$ and $\delta\dot{P}_c$, with volume derivatives eliminated.*

The final form of the variational equations obtained using the above procedure is given in Table 1, excluding the equation $\delta\dot{h} = -\delta w$. A detailed discussion of the physical significance of the various terms appearing in these equations is given in a later section. The purpose here is to present the result and to demonstrate that the stability information is correctly calculated using this procedure. In order to verify this procedure, stability results have been obtained for trunk flow rates $W_{tr} = 757$ lb/min (just prior to ground contact), 758 lb/min (just after ground contact), 840 lb/min (well after ground contact, vehicle still unstable), and 950 lb/min (well after ground contact, vehicle stable). In each case, the required partial derivatives were calculated using the tabular geometric trunk data generated in the original Boeing numerical analysis, the first two equations in Table 1 were solved simultaneously, and the eigenvalues of the resulting Jacobian matrix were computed. The results are summarized in Table 2, in which are shown the stability matrices and eigenvalues calculated as described above; for comparison, the eigenvalues obtained in the Boeing numerical work are also shown. Agreement is seen to be good, indicating that the present technique produces essentially the same results as a numerical variational procedure. This is not surprising; the details have been presented mainly to ensure that no mistakes were made in the calculation of the system matrices.

For each operating condition the complex conjugate eigenvalues describe the plunge motion of the vehicle. The additional real, negative eigenvalues represent highly damped subsidences which derive from the pressure response characteristics of the system.

*In the original Boeing numerical work reported in Ref. 1, the volumes V_c and V_t were included as states and modeled using a first order lag. Thus, there were six states in the Boeing linearized model.

TABLE I
LINEARIZED VARIATION EQUATIONS

TRUNK PRESSURE, EQUATION (1)

$$\delta \dot{P}_t \left[1 + \frac{k P_{t0}}{A_{s0}} \frac{\partial A_s}{\partial P_t} \right] + \delta \dot{P}_c \left[\frac{k P_{t0}}{A_{s0}} \frac{\partial A_s}{\partial P_c} \right] = \left[\frac{k P_{t0}}{A_{s0}} \frac{\partial A_s}{\partial h} \right] \delta W$$

$$+ \left(\frac{kRT}{V_{t0}} \right) \left\{ -\delta P_t \left[\frac{W_{tr}}{P_{t0}} + \frac{W_{tc0}}{2 \Delta P_{t0}} + \frac{W_{tc0}}{2(P_{t0} - P_{c0})} \right] + \delta P_c \left[\frac{W_{tc0}}{2(P_{t0} - P_{c0})} \right] \right\}$$

CUSHION PRESSURE, EQUATION (2)

$$\delta \dot{P}_c \left[1 + \frac{k P_{c0}}{V_{c0}} \frac{\partial V_c}{\partial P_c} \right] + \delta \dot{P}_t \left[\frac{k P_{c0}}{V_{c0}} \frac{\partial V_c}{\partial P_t} \right] = \left[\frac{k P_{c0}}{V_{c0}} \frac{\partial V_c}{\partial h} \right] \delta W$$

$$+ \left(\frac{kRT}{V_{c0}} \right) \left\{ \delta P_t \left[\frac{W_{tc0}}{P_{t0}} + \frac{W_{tc0}}{2(P_{t0} - P_{c0})} - \frac{W_{c0}}{Z_{g0}} \frac{\partial Z_g}{\partial P_t} \right] \right.$$

$$\left. - \delta P_c \left[\frac{W_{tc0}}{P_{c0}} + \frac{W_{tc0}}{2 \Delta P_{t0}} + \frac{W_{tc0}}{2(P_{t0} - P_{c0})} + \frac{W_{c0}}{Z_{g0}} \frac{\partial Z_g}{\partial P_c} \right] - \delta h \left[\frac{W_{c0}}{(h - h_{c0})} + \frac{W_{c0}}{Z_{g0}} \frac{\partial Z_g}{\partial h} \right] \right\}$$

PLUNGE MOTION, EQUATION (3)

$$\delta \dot{W} = \frac{-2D}{M_{cg}} \left\{ \delta P_t \left[\frac{\Delta P_{t0}}{L_{30}} \frac{\partial L_3}{\partial P_t} + L_{30} + \Delta P_{c0} \frac{\partial Y_0}{\partial P_t} \right] + \delta W \left(L_{30} D_{mp} \right) \right.$$

$$\left. + \delta P_c \left[\frac{\Delta P_{t0}}{L_{30}} \frac{\partial L_3}{\partial P_c} + (Y_a + Y_0) + \Delta P_{c0} \frac{\partial Y_0}{\partial P_c} \right] + \delta h \left[\frac{\Delta P_{t0}}{L_{30}} \frac{\partial L_3}{\partial h} + \Delta P_{c0} \frac{\partial Y_0}{\partial h} \right] \right\}$$

() = 0 BEFORE GROUND CONTACT

() = 0 AFTER GROUND CONTACT

STABILITY TECHNIQUE VERIFICATION

$$W_{kr} = 757 \text{ lb/min}$$

$$\begin{Bmatrix} \delta r \\ \delta p \\ \delta w \\ \delta h \end{Bmatrix} = \begin{bmatrix} 411.5 & -975.3 & 6.52 & -2303 \\ 273.3 & -633.7 & 4.20 & -1484 \\ 6.109 & -45.13 & 0 & 0 \\ 0 & 0 & -1 & 0 \end{bmatrix} \begin{Bmatrix} \delta r \\ \delta p \\ \delta w \\ \delta h \end{Bmatrix}$$

$$[A] = \begin{bmatrix} -29.2 & 2.806 & 6.855 & -610.7 \\ -6.073 & -12.1 & 3.977 & -625.2 \\ -9.063 & -11.43 & 0 & 52.55 \\ 0 & 0 & -1 & 0 \end{bmatrix}$$

$$W_{kr} = 840 \text{ lb/min}$$

$$[A] = \begin{bmatrix} -28.06 & -1.26 & 6.45 & -455.8 \\ -1.17 & -21.07 & 2.55 & -557.7 \\ -11.28 & -4.43 & -1.001 & 61.02 \\ 0 & 0 & -1 & 0 \end{bmatrix}$$

$$W_{kr} = 950 \text{ lb/min}$$

$$[A] = \begin{bmatrix} -27.61 & -16.1 & 4.7 & -178.4 \\ 3.78 & -51.9 & .035 & -188.8 \\ -12.34 & 5.6 & -2.312 & 87.94 \\ 0 & 0 & -1 & 0 \end{bmatrix}$$

EIGENVALUE COMPARISON

W_{kr}
757
758
840
950

ABOVE MATRICES

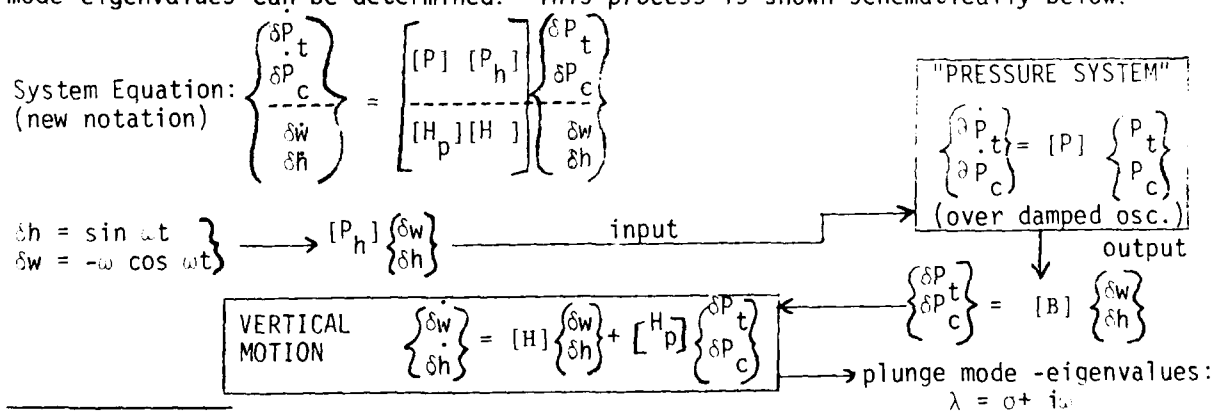
-2.1 ± 12.43i, -25.2, -192.8
4.81 ± 20.43i, -19.3, -31.6
3.23 ± 16.97i, -21.7, -32.1
-2.21 ± 9.8i, -28.1, -49.5

BOEING NUMERICAL

-2.15 ± 13.2i, -19.6, -98.2
5.61 ± 20.79i, -14.2, -29.5
2.30 ± 17.44i, -16.4, -28.1
-2.81 ± 9.48i, -19.9, -35.9

b. "Describing Function" Analysis*

A simplification of the technique presented in the preceding subsection is possible by taking into account the nature of the present system behavior. If we consider the case where the vertical motion is frozen, then small deviations from equilibrium in trunk and/or cushion pressures will decay exponentially (and very rapidly) back to the equilibrium level, as described approximately by the real, negative eigenvalues resulting for the system matrices given in Table 2. Thus, qualitatively the pressure response is similar to that of an overdamped mechanical oscillator. The pressure and plunge motions can be partially decoupled by considering the process to occur in the following sequence: (1) assume that the plunge motion is approximately simple harmonic, $h = \sin \omega t$; (2) this plunge motion and the associated velocity $\dot{h} = \omega \cos \omega t$ are then considered to provide a harmonic forcing of the cushion and trunk pressures, as defined by the terms a_{13} , a_{14} , a_{23} , and a_{24} in the linearized equation (12); (3) responding to this input as would an overdamped oscillator, the pressure output will also be harmonic with some gain and phase shift relative to the input; (4) the output pressures P_c and P_t may then each be considered to be linearly related to altitude h and velocity \dot{h} , for example, $P_c = Sh + C\dot{h}$; and (5) the altitude/velocity dependence of P_c and P_t then serve to define the stiffness and damping in the linearized equation of plunge motion. At this point, the plunge mode eigenvalues can be determined. This process is shown schematically below:



*So called because the approach is similar to that used in analyzing nonlinear control systems.

Mathematically, the results obtained using the above procedure are now summarized. Starting with the pressure equations,

$$\dot{p}_t = a_{11}p_t + a_{12}p_c + a_{13}w + a_{14}h \quad (16)$$

$$\dot{p}_c = a_{21}p_t + a_{22}p_c + a_{23}w + a_{24}h \quad (17)$$

we differentiate equation (17) with respect to time and then eliminate p_t from the result, yielding a second order differential equation for the cushion pressure p_c ,

$$\begin{aligned} \ddot{p}_c - (a_{11} + a_{22})\dot{p}_c + (a_{11}a_{22} - a_{21}a_{12})p_c = h [a_{21}a_{14} - a_{11}a_{24}] \\ + a_{23}\dot{w} + w [a_{21}a_{13} - a_{11}a_{23} - a_{24}] \end{aligned} \quad (18)$$

Now, assuming the altitude to vary harmonically, $h = \sin \omega t$ (and so $\dot{h} = -\dot{h} = -\omega \cos \omega t$), equation (18) takes the form

$$\ddot{p}_c - T\dot{p}_c + \Delta p_c = K_s \sin \omega t + K_c \cos \omega t \quad (19)$$

$$\text{where } K_s = a_{21}a_{14} - a_{11}a_{24} + a_{23}\omega^2$$

$$K_c = \omega(a_{24} + a_{11}a_{23} - a_{21}a_{13})$$

$$T = a_{11} + a_{22}$$

$$\Delta = a_{11}a_{22} - a_{21}a_{12}$$

Note that T and Δ are the trace and determinant of the pressure system $[P]$ submatrix defined at the beginning of this section. Thus, in this decoupling procedure the real, negative eigenvalues λ_1 and λ_2 are given approximately by $\lambda_1\lambda_2 = \Delta$ and $\lambda_1 + \lambda_2 = T$. Equation (19) shows that a given vertical motion is in general amplified and phase shifted before acting as input to the pressure system. The above equation can be solved to give the steady state pressure response to the harmonic vertical motion,

$$p_c = C \cos \omega t + S \sin \omega t.$$

This may be rewritten in terms of h and \dot{h} as

$$P_c = Sh + \frac{C}{\omega} \dot{h} \quad (20)$$

Also,

$$P_t = \frac{h}{a_{21}} [-C\omega - a_{22}S - a_{24}] + \frac{\dot{h}}{a_{21}} [S - \frac{a_{22}C}{\omega} + a_{23}] \quad (21)$$

where

$$S = \frac{1}{D} [(D-\omega^2)K_s - T\omega K_c]$$

$$C = \frac{1}{D} [(D-\omega^2)K_c + T\omega K_s]$$

$$\text{and } D = (\Delta-\omega^2)^2 + (T\omega)^2.$$

The output of the pressure system, expressed as equations (20) and (21), is now put back into the vertical motion equation, and the result is written in the form

$$\ddot{h} + D\dot{h} + Fh = 0 \quad (22)$$

where the damping term D and frequency term F are

$$D = \frac{a_{31}}{a_{21}} (S - \frac{a_{22}C}{\omega} + a_{23}) + \frac{a_{32}C}{\omega} - a_{33}$$

$$F = \frac{a_{31}}{a_{21}} (-C\omega - a_{22}S - a_{24}) + a_{32}S + a_{34}$$

The complex eigenvalues corresponding to the vertical motion are then

$$\lambda_{3,4} = -\frac{D}{2} \pm i [F - D^2/4]^{1/2}. \quad (23)$$

Thus, if $D > 0$, the vertical motion is stable and if $D < 0$ it is unstable. In practice, the plunge mode eigenvalues are calculated iteratively until the input frequency ω equals that obtained from the solution to equation (22). This formulation is useful because the plunge motion is now described as that of a freely vibrating damped (or undamped) oscillator.

In order to verify this technique as a means of assessing the various parameter influences on vehicle stability, the plunge mode eigenvalues as calculated above are compared below to those given in Table 2 for the same four trunk flow rates considered earlier.

Simplified Model Eigenvalue Comparison

W_{tr} (lb/min)	Approximate: Equation (23)	Exact (Table 2)
757	$-1.8 \pm 12.4i$	$-2.1 \pm 12.43i$
758	$6.55 \pm 18.7i$	$4.81 \pm 20.43i$
840	$3.15 \pm 16.6i$	$3.23 \pm 16.97i$
950	$-2.08 \pm 9.8i$	$-2.21 \pm 9.8i$

The agreement is good, indicating that the partial decoupling procedure used here is valid. Use of this technique to analyze the cause of the unstable model behavior is made in the following section.

3. Analysis of Model Stability Behavior

a. System equations

In this section, the observed stability behavior is explained in some detail, first for the grossly destabilizing effect of first ground contact and then the stabilizing influence of further increases in trunk flow rate. We start by considering the variational vertical force equation appearing in Table 1, which is rewritten in the form (with the δ 's dropped)

$$\begin{aligned}
 \ddot{h} = & \frac{2D}{M} \left\{ P_t \left[\underbrace{\Delta P_{to} \frac{\partial L_3}{\partial P_t}}_{4.05} + \underbrace{L_{30}}_{-2.86} + \underbrace{\Delta P_{co} \frac{\partial Y_o}{\partial P_t}}_{4.69} \right] + P_c \left[\underbrace{\Delta P_{to} \frac{\partial L_3}{\partial P_c}}_{-8.99} + \underbrace{(Y_a + Y_o)}_{15.2} \right] \right. \\
 & \left. + \underbrace{\Delta P_{co} \frac{\partial Y_o}{\partial P_c}}_{10.42} \right\} - \dot{h} \left[\underbrace{L_{30} D_{MP}}_0 \right] + h \left[\underbrace{\Delta P_{to} \frac{\partial L_3}{\partial h}}_{-14.02} + \underbrace{\Delta P_{co} \frac{\partial Y_o}{\partial h}}_{6.24} \right] = 0 \quad (24)
 \end{aligned}$$

Terms underlined with a squiggly line are nonzero only after trunk/ground contact. The magnitudes of the various partial derivative terms in L_3 and Y_o are noted where these terms appear in equation (24). Values above the corresponding term represent

the case just prior to ground contact ($W_{tr} = 757$ lb/min), while those below refer to just after ground contact ($W_{tr} = 758$ lb/min). The changes in the partial derivatives reflect the direct sensitivity of L_3 and Y_0 to altitude following trunk/ground contact.

The various terms in equation (24) describe the manner in which the net vertical force on the vehicle changes due to small changes in the four states. The \dot{h} term is due to direct damping as modeled in Reference 1; the damping force is proportional to the area of trunk ground contact $2DL_3$. Since L_3 is essentially zero just after ground contact, as well as before, this direct damping model has no influence on the system stability until L_3 becomes appreciable, as it does for higher trunk flow rates.

All of the terms, other than the direct damping, are related to the net pressure force on the vehicle and how this force changes as P_c , P_t , and h are varied slightly. Physically, there are two distinct effects: (1) change in vertical force due to changes in pressures; and (2) changes in vertical force due to changes in the areas over which the pressures act. The latter of these is a result of the alteration in trunk shape, with attendant area change, which accompanies a change in pressure ratio, P_r and altitude ratio Z_r . The former effect is what would be observed if the trunk were completely rigid.

Pressure force changes due to area change are governed by the partial derivative terms in equation (24). For example, prior to ground contact $\partial Y_0 / \partial P_c = 6.41$ in./psi. This indicates that if P_c were increased slightly, the trunk would tend to be pushed outward, thus increasing the distance Y_0 to the horizontal tangency point and, therefore, also increasing the cushion area (and net vertical force). As another example, considering the influence of ground contact width L_3 , we see that following ground contact $\partial L_3 / \partial P_t = 4.05$ in./psi. Physically, as P_t is increased slightly, the trunk is pushed inward and down, increasing the contact width

and hence the area over which the trunk pressure P_t acts. The remaining partial derivatives may be interpreted in an analogous fashion and all are physically reasonable. The magnitudes of the various area change (i.e., partial derivative) effects in equation (24) indicate that the sensitivity of trunk shape to trunk and cushion pressures and altitude is very important in determination of the net pressure force characteristics.

Combining the various coefficients appearing in equation (24), the equation of vertical motion for the cases before and after ground contact is given by

$$\ddot{h} + 6.109 P_t - 45.13 P_c = 0 \quad (\text{before contact}) \quad (25)$$

$$\ddot{h} - 9.06 P_t - 11.43 P_c + 52.5h = 0 \quad (\text{after contact})$$

The change in coefficients is due mainly to the appearance of the contact width L_3 effects of the ground contact and to a lesser extent the change in Y_0 behavior. These changes are not necessarily the cause of the unstable behavior and are viewed at this point as merely indicating to what degree the trunk and cushion pressures contribute to the net vertical force change. Note also that the net effect of the altitude sensitivities of Y_0 and L_3 after contact is to stiffen the system and these effects should result mainly in higher plunge mode frequency after ground contact.

To properly assess vehicle stability we must look at the variational forms of the pressure equations. This will be done in much the same way as above and then the vertical motion and pressures will be viewed as they interact together. We first consider the variational equation for the trunk pressure, which from Table 1 is (with δ 's dropped)

$$\begin{aligned} \dot{P}_t \left[1 + \frac{3.313}{1.783} \frac{kP_{to}}{A_{so}} \frac{\partial A_s}{\partial P_t} \right] + \dot{P}_c \left[\frac{-5.14}{-1.742} \frac{kP_{to}}{A_{so}} \frac{\partial A_s}{\partial P_c} \right] = \\ \left(\frac{kRT}{V_{to}} \right) \left\{ -P_t \left[\frac{W_{tr}}{P_{to}} \frac{7.44}{2\Delta P_{to}} + \frac{W_{tao}}{2\Delta P_{to}} \frac{1.09}{2(P_{to} - P_{co})} + \frac{W_{tco}}{2(P_{to} - P_{co})} \frac{3.11}{2(P_{to} - P_{co})} \right] \right. \\ \left. + P_c \left[\frac{W_{tco}}{2(P_{to} - P_{co})} \frac{3.11}{2(P_{to} - P_{co})} \right] \right\} + w \left[\frac{kP_{to}}{A_{so}} \frac{\partial A_s}{\partial h} \right] \end{aligned} \quad (26)$$

In this equation, terms involving equilibrium flow rates describe the variations in \dot{P}_t resulting from pressure variation and its effect on the various air flows given in equations (7) - (10). For example, a slight increase in cushion pressure P_c will decrease the trunk to cushion flow W_{tc} , which will cause P_t to rise (i.e., $\dot{P}_t > 0$). Likewise, an increase in trunk pressure P_t will cause an increase in both trunk to cushion and trunk to atmosphere flows W_{tc} and W_{ta} which will, in turn, cause P_t to drop (i.e., $\dot{P}_t < 0$). These effects are identical just before and just after ground contact, so the instability cannot be attributed directly to them.

The terms in equation (26) which involve partial derivatives of trunk cross sectional area A_s with respect to P_t , P_c , and h arise from the rate of change of volume effect in equation (1) (since $V_t = 2D A_s$, \dot{V}_t/V_t was replaced by \dot{A}_s/A_s in this equation). This effect is a significant one and changes noticeably before and after ground contact. Combining the coefficients in equation (26) results in the following for the variational version of equation (1) (δ notation dropped) for the cases before and after ground contact.

$$\begin{aligned} 3.31 \dot{P}_t - 5.14 \dot{P}_c &= -41.48 P_t + 26.08 P_c \quad (\text{before contact}) \\ 1.783 \dot{P}_t - 1.742 \dot{P}_c &= -41.48 P_t + 26.08 P_c + 5.3w \quad (\text{after contact}) \end{aligned} \quad (27)$$

The equation (2) defining cushion pressure rate of change \dot{P}_c may be viewed in a manner similar to the above. The variational form of this equation from Table 1 is

$$\begin{aligned} \dot{P}_c \left[1 + \frac{kP_{co}}{V_{co}} \frac{\partial V_c}{\partial P_c} \right] + \dot{P}_t \left[\frac{kP_{co}}{V_{co}} \frac{\partial V_c}{\partial P_t} \right] &= \left[\frac{kP_{co}}{V_{co}} \frac{\partial V_c}{\partial h} \right] w \\ &+ \left(\frac{kRT}{V_{co}} \right) \left\{ P_t \left[\frac{W_{tco}}{P_{co}} + \frac{W_{tco}}{2(P_{to} - P_{co})} - \frac{W_{cao}}{Z_{go}} \frac{\partial Z_g}{\partial P_t} \right] - P_c \left[\frac{W_{tco}}{P_{co}} + \frac{W_{tco}}{2\Delta P_{co}} \right] \right. \\ &+ \left. \frac{W_{tco}}{2(P_{to} - P_{co})} \frac{W_{cao}}{Z_{go}} \frac{\partial Z_g}{\partial P_c} \right] - h \left[\frac{W_{cuo}}{(h - h_{cu})} + \frac{W_{cao}}{Z_{go}} \frac{\partial Z_g}{\partial h} \right] \left. \right\} \end{aligned} \quad (28)$$

In equation (28), the trunk to cushion flow rate W_{tco} effect is similar to the equilibrium flow effects in equation (26). For example, an increase in trunk pressure P_t will increase the trunk to cushion flow rate, which will cause P_c to increase (i.e., $\dot{P}_c > 0$). Likewise, an increase in cushion pressure will decrease W_{tc} , causing \dot{P}_c to be negative. The partial derivatives of cushion volume V_c arise from the volume rate of change \dot{V}_c/V_c term in equation (2). They are much larger in magnitude than the corresponding terms in the trunk pressure equation (26) because the cushion frontal area $2[Z_o(Y_a + Y_o) - A_{cv}]$ increases much more rapidly than does the trunk area A_s when a pressure variation occurs so as to push the trunk outward (i.e., increase in P_c or decrease in P_t).

A significant difference between the cushion and trunk pressure equations is in the cushion to atmosphere flows W_{ca} and W_{cu} . Unlike the flows which govern trunk pressure rate of change, both of these flows are sensitive to altitude. In addition, the cushion/atmosphere flow W_{ca} is very sensitive to pressure change. For example, an increase in cushion pressure will cause the trunk to be pushed outward and upward, increasing the gap (Z_{gap}) between the trunk and the ground, in turn increasing the flow rate W_{ca} ; this will cause the cushion pressure to drop (i.e., $\dot{P}_c < 0$) much more quickly than would occur for a rigid trunk. An increase in trunk pressure will cause a reduction in Z_{gap} , a reduction in W_{ca} and, hence, an increase in P_c (i.e., $\dot{P}_c > 0$). For both of these flows, the influence of pressure variations on the pressure portion of the flow rates will also appear, but this effect is small compared to the altitude sensitivity. We further note that the influence of pressure change on the cushion end flow W_{cu} variation is small since, in the present model, the end elements are frozen and high enough off the ground so that they never contact it. Thus, when the trunk-ground contact condition occurs, all of the numerically large terms involving the partial derivatives of Z_{gap} disappear, since W_{ca} is then zero. Working out the coefficients in equation (28) before and after ground contact leads to

$$-20.65 \dot{P}_t + 46.89 \dot{P}_c = 4318 P_t - 9575 P_c + 62.4 w - 22049 h \quad (\text{before contact})$$

(29)

$$-8.86 \dot{P}_t + 20.7 \dot{P}_c = 133 P_t - 275.3 P_c + 21.6 w - 7531 h \quad (\text{after contact})$$

Here the gross difference between the two cases is clearly in evidence.

b. Stability assessment

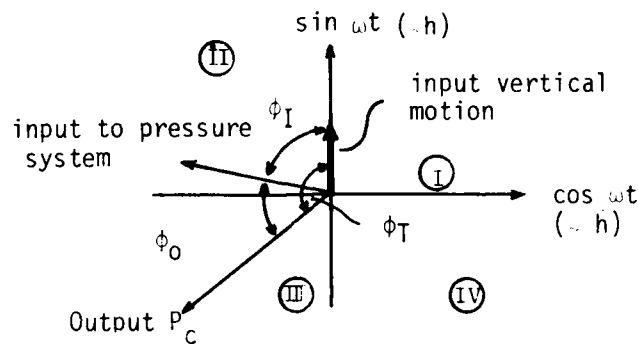
Here we apply the "describing function" approach to obtain a qualitative description of the basic stability behavior before and after ground contact. This is done through study of the phasing relationships which occur when a sinusoidal vertical motion excites a sinusoidal steady state pressure response which, in turn, is fed back into the vertical motion equation (25). There are two phase shifts of interest in this analysis. The first occurs as in equation (19); i.e., a harmonic vertical motion $h = \sin \omega t$ is amplified and phase shifted before its input to the cushion pressure equation. If we write the right-hand side of equation (19) as $K_s \sin \omega t + K_c \cos \omega t = A \sin (\omega t - \phi_I)$, then the input amplification $A_I = (K_s^2 + K_c^2)^{1/2}$ and the input phase shift $\phi_I = \tan^{-1} (-K_c/K_s)$. The I subscript indicates input. A second amplification and phase shift occur as this input is fed through the pressure system. The cushion and trunk pressure amplification and phase shift are obtained from equations (20) and (21) as

$$A_o = 1/\{ (\Delta - \omega^2)^2 + (T\omega)^2 \}^{1/2} ; \quad \phi_o = \tan^{-1} \left(\frac{-T\omega}{\Delta - \omega^2} \right)$$

where the o subscript indicates pressure system output. The total phase shift, i.e. the phase difference between the input motion $h = \sin \omega t$ and the output cushion pressure will then be $\phi_T = \phi_I + \phi_o$. Note that this result refers to cushion pressure; the trunk pressure phase angle will be only slightly different.

To interpret the stability behavior using these phasing relations, consider the effect of trunk and cushion pressures on the vertical motion as given by equations (25). It turns out that the amplitude and phase of P_c and P_t are about equal,

so it is sufficient to consider the effect of only the cushion pressure P_c . Equations (25) show that the plunge motion will be both statically and dynamically stable if P_c as defined in equation (20) is proportional to $-h$ and to $-\dot{h}$. This will ensure that the plunge motion damping and frequency terms D and F in equation (22) both be positive. The stability may, therefore, be assessed directly from a graph of the phase angle characteristics as sketched below:



The vehicle vertical motion $h = \sin \omega t$ is plotted along the vertical direction, and vehicle velocity \dot{h} along the horizontal direction, positive to the right. The input to the cushion pressure equation and the resulting output are also shown schematically. For static and dynamic stability the output P_c must lie in the third quadrant.

Results of the phasing behavior for the cases before and after ground contact are shown in Figure 5 with pertinent numerical values indicated at the top of the Figure. The pressure system inputs are seen to be essentially the same in phase and comparable in magnitude before and after ground contact. Both of these inputs are dominated by the altitude sensitivity of the flows W_{ca} and W_{cu} prior to ground contact and W_{cu} after contact; these appear in the cushion pressure variational equation (28). The other altitude and velocity effects in equation (26) and (28) are relatively insignificant.

① $h = \sin \omega t$

②
$$\ddot{P}_C - T \dot{P}_C + \Delta P_C = K_S \sin \omega t + K_C \cos \omega t$$

(-222)	(5782)	(-18034)	(-19989)
(-41.3)	(370.4)	(-12956)	(-13993)

BEFORE CONTACT



AFTER CONTACT

— AFTER CONTACT
 — BEFORE CONTACT

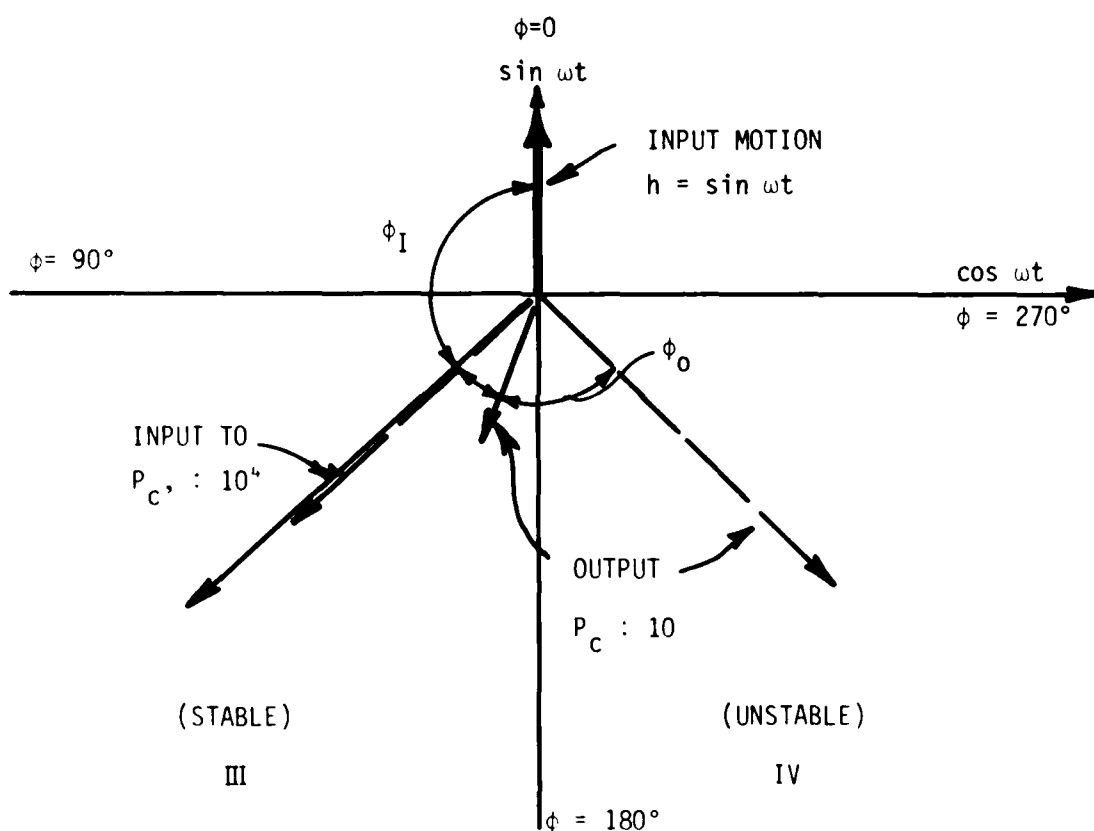


Figure 5 - Pressure Phasing Relations Before and After Ground Contact

The most noticeable difference occurs in the cushion pressure output; before ground contact the cushion pressure output is phase shifted relative to the input by only a small amount while, after ground contact, the phase shift is nearly 90°, and the amplification is also greater. The important result is that the output cushion pressure ends up in the third quadrant of Figure 5 before ground contact and in the fourth quadrant after contact. To see how this influences the stability, note from equation (25) that for stability the net contributions from P_c and P_t must be proportional to $-\dot{h}$ so that $D > 0$. This is the case if the output pressures lie in quadrant III but not in quadrant IV, for which the pressure contributions will be proportional to $+\dot{h}$.

The reason for the phase shift differences may be seen clearly by considering the cushion pressure response to be that of an overdamped mechanical oscillator subjected to a simple harmonic input. Equation (19) is thus considered in the form

$$\ddot{P}_c - \begin{matrix} -222 \\ -41.3 \end{matrix} T P_c + \begin{matrix} 5782 \\ 370 \end{matrix} \Delta P_c = \sin \omega t \quad (30)$$

Numbers listed above and below the T and Δ coefficients are for before and after ground contact, respectively. Recall that T and Δ define the "pressure system;" i.e., they represent completely the pressure response for the case of frozen vertical motion. The real, negative eigenvalues which describe this response before and after ground contact are as follows: before contact, we have $\lambda_{1,2} = -30, -212$ while, after contact, $\lambda_{1,2} = -13.2, -28.1$. These results are only approximate since they are calculated using the partial decoupling procedure involved in the "describing function" analysis. However, the results of Table 2 indicate that these approximate values are reasonably accurate. The critical damping ratios ζ associated with the above system before and after ground contact are given by $\zeta = -T/2 \sqrt{D}$ so that $\zeta = 1.46$ before ground contact and $\zeta = 1.073$ after ground contact. The large differences

in the magnitudes of T and Δ before and after ground contact are a result of the disappearance after contact of the cushion to atmosphere flow W_{ca} , whose altitude sensitivity prior to ground contact dominates the pressure system. Thus, following ground contact, the pressure system is affected only by the trunk to cushion and trunk to atmosphere flow pressure sensitivities. The effect of these characteristics on output cushion pressure may be noted by inspection of the steady state solution to equation (30),

$$P_c = \frac{\sin(\omega t - \phi)}{\left\{ \left(1 - \frac{\omega^2}{\Delta^2}\right)^2 + \left(\frac{T\omega}{\Delta}\right)^2 \right\}^{1/2}} ; \phi = \tan^{-1} \left(\frac{-T\omega}{\Delta - \omega^2} \right)$$

Now, before ground contact, the product Δ of the real negative eigenvalues is very large when compared to the square of the frequency $\omega \cong 12.4/\text{sec}$ of the vertical oscillatory motion. Thus, the resulting motion is analogous to the forced response of an overdamped oscillator subjected to a harmonic input whose frequency is well below the undamped natural frequency of the oscillator. The attendant output phase lag is relatively small. On the other hand, after ground contact occurs, the product of negative, real eigenvalues Δ is very close in magnitude to the square of the oscillator undamped natural frequency $\omega \cong 20/\text{sec}$. Effectively, the oscillator is being forced at a near resonant condition and the output phase lag will be close to 90° . This type of result will occur whenever the product of real eigenvalues is close to the square of the frequency of vertical motion. It is important to note here that the large, real eigenvalues characterizing the pressures before ground contact are due almost entirely to the sensitivity of the cushion to atmosphere flow W_{ca} to altitude variation. When this effect is removed at ground contact, the pressure response is considerably more sluggish. The W_{ca} /altitude sensitivity is in turn a result of the sensitivity of trunk geometry (specifically, the vertical movement of the lowest point on the trunk) to changes in trunk and cushion pressures. Thus, the importance of an accurate trunk shape model is evident.

One would tend to infer from the above that the instability is a result of changes in the "pressure system" which result in an effective resonant excitation of the pressures with attendant large phase lag. However, if we look at the dynamic behavior which occurs when the trunk flow rate W_{tr} is increased, we see that this is not really the case. Inspection of Table 2 shows that, at flow rates of $W_{tr} = 840$ lb/min and 950 lb/min, the pressure system, as well as the input to the system, have not changed very much when compared to the case $W_{tr} = 758$ lb/min. Nevertheless, the stability characteristics are altered substantially. This appears to be due largely to the shift in the cushion pressure sensitivity term a_{32} in the vertical force equation, which changes sign as the flow rate is increased to 950 lb/min. This is a result of combined decrease in the cushion width Y_0 parameter and pressure ratio P_r . The result is that the cushion pressure force variation is dominated by the area change (decrease) due to contact width L_3 sensitivity to cushion pressure variation. In essence, at this operating condition, a small increase in cushion pressure δP_c actually results in a decrease in vertical pressure force. Thus, although the pressure system output is not significantly different than for lower trunk flow rates, the effect on the vertical motion is altered.

The above results indicate that the stability behavior involves a relatively complex interaction of three things:

- (1) the manner in which a simple harmonic altitude oscillation of the vehicle serves to force the pressure system; for the present system and operating conditions this input is dominated by the cushion to atmosphere flows W_{ca} and W_{cu} .
- (2) The pressure "system" itself, which governs the pressure response to a given altitude input; the difference in response for the before/after contact cases is a result of removal from the pressure system of the pressure/altitude sensitivities to cushion/atmosphere flow W_{ca} which occurs at ground contact.

- (3) The manner in which the output pressures are converted to forces acting on the vehicle; this is largely responsible for the gradual stabilizing tendency of increased trunk flow rate as the cushion planform area sensitivity overcomes the direct pressure sensitivity.

The above factors appear to govern the plunge mode stability. Isolation of these factors, however, does not really uncover a physical source of the energy increase which accompanies unstable motion. It seems that the present phenomenon is similar to the classical self-excited vibration of systems excited by a unidirectional energy source as occurs in flow-induced vibration and wheel shimmy, for example. In this case, the unidirectional energy source is the power required to produce the input trunk flow W_{tr} . Apparently, depending on system properties as discussed previously, the vehicle motion may absorb energy from this input.

The system stability behavior may be changed by altering any or some of the three characteristics described above. This is not necessarily a simple procedure, since it may be difficult to alter the system in such a way as to affect only one of the above properties. The effect of altering specific system properties on vehicle stability, with emphasis on determining a way to eliminate or alleviate the instability, is discussed in the following section. Then an assessment of the adequacy of the present trunk geometry model is made.

Before going into these areas, a brief digression is made to show the influence of the damping model on stability. As noted in equation (3), the damping force is proportional to the total area of trunk/ground contact $2DL_3$ with the proportionality constant $D_{MP} = .24 \text{ lb sec/ft}$ in the present study. We also note from the variational form of the vertical motion equation, as given in Table 1, that the damping term appears as a_{33} in the system matrices of Table 7, specifically

$$a_{33} = \frac{-2D}{M} L_3 D_{MP}$$

Finally, note that in the describing function result given by equations (22) and (23), this damping term a_{33} directly influences only the real part of the plunge mode eigenvalue. In fact, equations (22) and (23) indicate that we may determine the stability behavior which would occur without damping by simply adding $-a_{33}/2$ to the real part which was obtained with damping included. A comparison of the cases with and without damping included will show the importance of the damping model in determining the overall stability behavior.

This comparison is shown in Figure 6 and is based on the original numerically determined stability information generated by Boeing Co. As expected for flow rates near first ground contact, $W_{tr} \cong 760$ lb/min, the difference is slight because the contact width L_3 is very small. As W_{tr} increases toward 950 lb/min, the effect is noticeable, although it is clear that the basic tendency of increased stability with trunk flow rate occurs regardless of whether damping is retained in the system equations. Thus, qualitatively the damping effect is not of paramount importance.

c. Parameter change effects on stability

In order to further assess the stability behavior, the effects of altering selected system parameters were investigated. This was done with the intent of determining the degree to which the aforementioned three effects on stability could be altered in such a way as to stabilize the vehicle.

(1) Effect of increased trunk flow coefficient.

It was noted previously that, mathematically, one reason for the unstable behavior following ground contact lay in the product of pressure system eigenvalues being of comparable magnitudes to the product of the conjugate plunge mode eigenvalues, resulting in a near 90° phase shift between pressure system input and output. One way to reduce this phase shift would be to alter system parameters so that the pressure system response is much quicker (i.e., characterized by larger

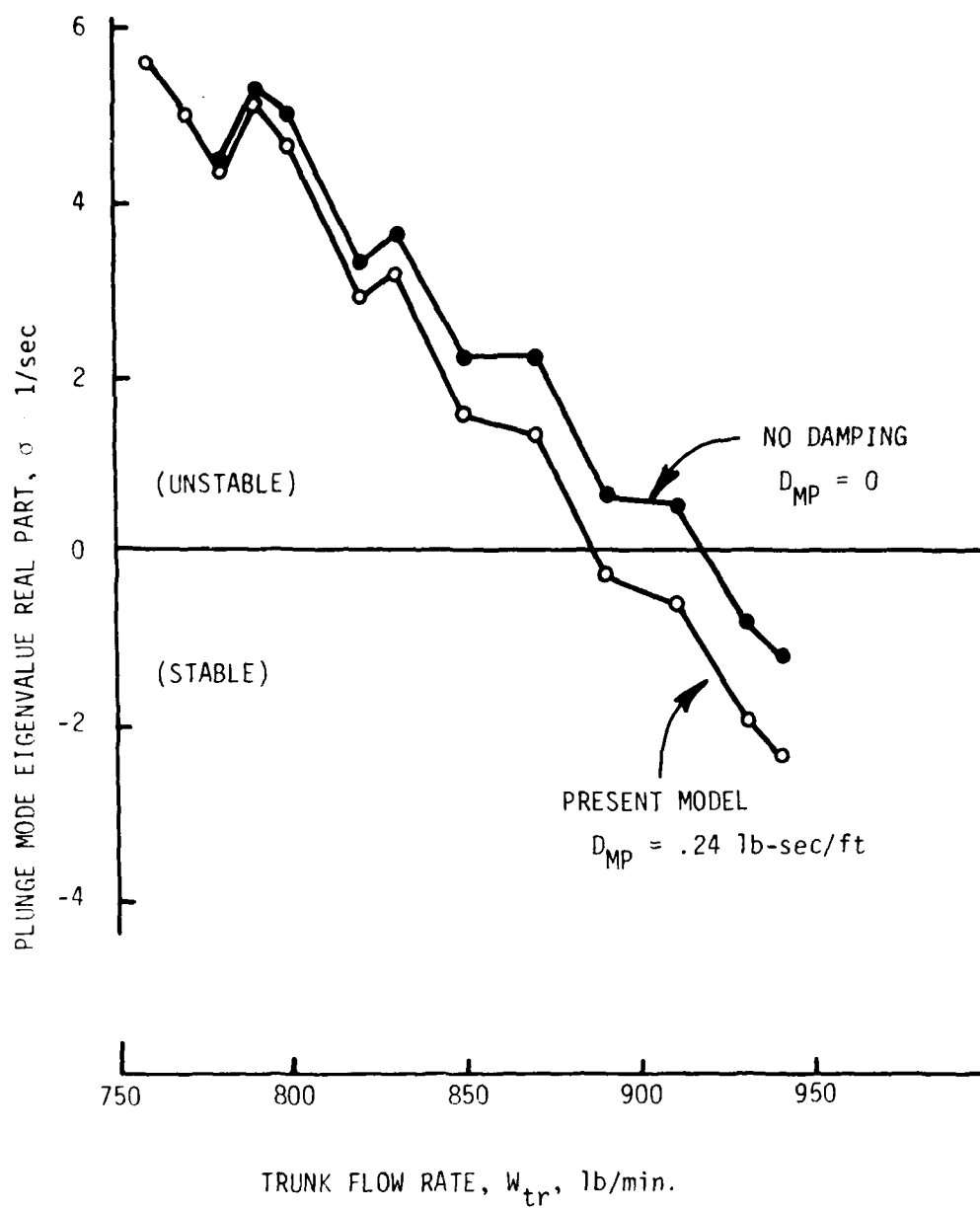


Figure 6 - Effect of Damping Model on Plunge Mode Stability

negative eigenvalues). Physically, this may be done by increasing the flow coefficients associated with the trunk to atmosphere and trunk to cushion flows W_{ta} and W_{tc} .

The effect of quicker pressure system response on stability following ground contact was assessed as follows: the system operating point was first chosen to be the same as before, and the flow coefficients CA_{ta} and CA_{tc} were doubled. This results in a required doubling of all flows, including W_{tr} and W_{cu} . The cushion end flow W_{cu} was doubled in such a way that its altitude sensitivity $W_{cu}/(h-h_{cu})$ remained the same as in the nominal system.

Insofar as the system stability matrix is concerned, these changes have the effect of doubling all terms in the pressure system submatrix $[P]$, while leaving everything else the same. The result is an approximate doubling of the pressure system eigenvalues which causes changes in both the pressure system input and output phasing (as well as amplitude). The overall effect on plunge mode stability is a noticeable improvement; the plunge mode eigenvalues are $\lambda_{3,4} = 2.75 \pm 18i$, as compared to $\lambda_{3,4} = 5.6 \pm 20.8i$ for the original system. In terms of phasing the change in pressure system shifts the input in a slightly destabilizing manner (i.e., increases ϕ_1) and the output in a stabilizing manner (i.e., decreases ϕ_0) such that the total phase shift ϕ_T is reduced and the stability improved.

Physically, the required doubling of all flows would result in a considerable increase in input power. This may represent an important design constraint. Nevertheless, the stabilizing tendency of quicker pressure system response appears substantial for this system.

(2) Effect of lowering operating pressure ratio.

Since the trunk geometry is very sensitive to pressure ratio P_r , calculations were made for an equilibrium pressure ratio $P_r = .3$ (the nominal operating value is $P_r = .45$) in order to deduce the dependence on P_r of the stability following ground

contact. Physically, the lower P_r results in the trunk being moved downward and inward and simultaneously moves the equilibrium altitude h upward. The operating pressures were changed to $P_c = 15.91$ psi and $P_t = 18.74$ psi. The operating flows at this pressure ratio are (in lb/sec) approximately $W_{tr} = 20.12$, $W_{tc} = 12.88$, $W_{ta} = 7.24$, $W_{cu} = 12.88$, and the equilibrium altitude $h = 4.0267$ ft (2.1 in higher than when $P_r = .45$). The system equations which result are summarized in Table 3. The various flow terms in the pressure equations are altered but not drastically. The most notable difference is in the cushion end flow W_{cu} altitude sensitivity effect, which is decreased in magnitude substantially. There are two reasons for this:

- (a) It was assumed that the trunk/cushion flow coefficient was unchanged, so that W_{tc} changed according to the altered equilibrium pressures P_c and P_t . Since at equilibrium following ground contact $W_{cu} = W_{tc}$, the W_{cu} flow coefficient had to be lowered to achieve this equality.
- (b) The end cushion gap $h-h_{cu}$ is relatively much larger due to upward movement of the equilibrium position. These effects combine to reduce the ratio $W_{cu}/(h-h_{cu})$ in the cushion pressure equation.

Application of the describing function approach for the case after ground contact yields a plunge mode eigenvalue of $\lambda = 1.1 \pm 14.4i$, which indicates a substantial improvement in vehicle stability. It is tempting to conclude that operating pressure ratio has a substantial influence on vehicle stability. However, as discussed in the following subsection, the lowered W_{cu} /altitude sensitivity, which arose here as a requirement of altered equilibrium pressure ratio, appears to be the dominant factor.

TABLE 3

LINEARIZED VARIATION EQUATIONS FOR REDUCED OPERATING PRESSURE RATIO

TRUNK PRESSURE, EQUATION (1)

$$\delta \dot{P}_t \left[1 + \overset{1.248}{\frac{\dot{h} P_{t0}}{A_{s0}}} \frac{\partial A_s}{\partial P_t} \right] + \delta \dot{P}_c \left[\overset{-1.926}{\frac{\dot{h} P_{t0}}{A_{s0}}} \frac{\partial A_s}{\partial P_c} \right] = \left[\overset{4.262}{\frac{\dot{h} P_{t0}}{A_{s0}}} \frac{\partial A_s}{\partial h} \right] \delta W$$

$$+ \left(\overset{7.835}{\frac{\dot{h} R T}{V_{t0}}} \right) \left\{ - \delta P_t \left[\overset{1.074}{\frac{W_{t0}}{P_{t0}}} + \overset{.896}{\frac{W_{t0}}{2 \Delta P_{t0}}} + \overset{2.276}{\frac{W_{t0}}{2(P_{t0} - P_{c0})}} \right] + \delta P_c \left[\overset{2.276}{\frac{W_{t0}}{2(P_{t0} - P_{c0})}} \right] \right\}$$

CUSHION PRESSURE, EQUATION (2)

$$\delta \dot{P}_c \left[1 + \overset{19.84}{\frac{\dot{h} P_{c0}}{V_{c0}}} \frac{\partial V_c}{\partial P_c} \right] + \delta \dot{P}_t \left[\overset{-5.65}{\frac{\dot{h} P_{c0}}{V_{c0}}} \frac{\partial V_c}{\partial P_t} \right] = \left[\overset{14.7}{\frac{\dot{h} P_{c0}}{V_{c0}}} \frac{\partial V_c}{\partial h} \right] \delta W$$

$$+ \left(\overset{48.85}{\frac{\dot{h} R T}{V_{c0}}} \right) \left\{ \delta P_t \left[\overset{.687}{\frac{W_{c0}}{P_{t0}}} + \overset{2.276}{\frac{W_{c0}}{2(P_{t0} - P_{c0})}} - \overset{.}{\frac{W_{c0}}{Z_{g0}}} \frac{\partial Z_g}{\partial P_t} \right] \right.$$

$$\left. - \delta P_c \left[\overset{.809}{\frac{W_{c0}}{P_{c0}}} + \overset{5.314}{\frac{W_{c0}}{2 \Delta P_{c0}}} + \overset{2.276}{\frac{W_{c0}}{2(P_{t0} - P_{c0})}} + \overset{.}{\frac{W_{c0}}{Z_{g0}}} \frac{\partial Z_g}{\partial P_c} \right] - \delta h \left[\overset{57.6}{\frac{W_{c0}}{(h - h_{cu})}} + \overset{.}{\frac{W_{c0}}{Z_{g0}}} \frac{\partial Z_g}{\partial h} \right] \right\}$$

PLUNGE MOTION, EQUATION (3)

$$\delta \dot{W} = \frac{-2D}{M_y} \left\{ \delta P_t \left[\overset{4.04}{\Delta P_{t0}} \frac{\partial L_3}{\partial P_t} + \overset{1.06}{L_{30}} + \overset{0}{\Delta P_{c0}} \frac{\partial Y_0}{\partial P_t} \right] + \delta W \left(\overset{0}{L_{30} D_{mp}} \right) \right.$$

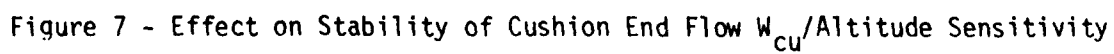
$$\left. + \delta P_c \left[\overset{4.04}{\Delta P_{t0}} \frac{\partial L_3}{\partial P_c} + \overset{-3.54}{(Y_a + Y_0)} + \overset{12.79}{\Delta P_{c0}} + \overset{1.212}{\Delta P_{c0}} \frac{\partial Y_0}{\partial P_c} \right] + \delta h \left[\overset{4.04}{\Delta P_{t0}} \frac{\partial L_3}{\partial h} + \overset{-16.14}{\Delta P_{c0}} \frac{\partial Y_0}{\partial h} \right] \right\}$$

() = 0 BEFORE GROUND CONTACT() = 0 AFTER GROUND CONTACT

(3) Effect of cushion end flow W_{cu} - altitude sensitivity.

As a result of the behavior discussed in subsection 2 above, the influence of cushion end flow W_{cu} characteristics on stability was next addressed. Physically, this flow is necessary following ground contact in order that the cushion pressure P_c remain below the trunk pressure P_t . In the present system model, the trunk end elements are modeled as rigid components whose lowermost point is h_{cu} from the center of mass ($h_{cu} = 45.64$ in nominally). The altitude sensitivity $W_{cu}/(h-h_{cu})$ appearing in the cushion pressure equation, Table 1, is very large because of the small gap $h-h_{cu}$ existing at equilibrium when the trunk first contacts the ground. This sensitivity can be decreased without altering the net equilibrium flow (and, hence, without altering any of the operating point parameters) by simultaneously decreasing h_{cu} and the flow coefficient in CA_{cu} [following equation (10)]. This has the effect of increasing the gap $h-h_{cu}$ while keeping the total flow area constant. Note that the limiting case $W_{cu}/(h-h_{cu}) \rightarrow 0$ is a physically reasonable one and represents a direct venting of cushion to atmosphere through a constant area orifice (i.e., not under the end elements).

The effect of decreased cushion flow/altitude sensitivity was assessed parametrically by reducing the $W_{cu}/(h-h_{cu})$ coefficient by varying amounts, leaving all other system parameters the same, and applying the describing function approach to calculate the plunge mode eigenvalues following trunk/ground contact. The resulting eigenvalues are shown in Figure 7 as a function of the factor K by which $W_{cu}/(h-h_{cu})$ was reduced. There is a substantial stabilizing tendency for $W_{tr} = 758$ lb/min, i.e. the first ground contact condition. In fact, if the end cushion flow were replaced by flow through a constant area orifice, the results for the three flow rates shown indicate that the vehicle would be stable for all conditions following trunk/ground contact.



There are several reasons for this behavior. We note first that altering only $W_{cu}/(h-h_{cu})$ by a certain factor K will alter the system matrix elements a_{14} and a_{24} by the same factor. Thus, the pressure system remains unchanged, but the input to the system is altered. Since the $W_{cu}/(h-h_{cu})$ sensitivity dominates the pressure system input, the resulting input is also reduced by K with approximately the same phasing as originally. The reduction in input magnitude causes a like reduction in pressure system output amplitude. Furthermore, these effects cause a noticeable lowering in the plunge mode frequency, Figure 7. This, in turn, reduces the amount of phase shift ϕ_0 produced by the pressure system, since the square of the input frequency ω^2 is then less than the product of eigenvalues of the pressure system; i.e., the system is being forced below its "resonant frequency." The combined reduction in phase shift and pressure output magnitudes, when put into equation (22) for vertical motion, result in a substantial improvement in stability. Similar trends are noted for the increased trunk flow of $W_{tr} = 840$ lb/min. For the case $W_{tr} = 950$ lb/min, there appears to be little effect of the W_{cu} /altitude sensitivity since, for these higher flow rates, the other system parameters have changed enough to alter the stability on their own.

The above discussion indicates that the dominant destabilizing influence for operation after first ground contact is the presence of the large cushion flow-altitude sensitivity, combined with the disappearance of the various sensitivities associated with the cushion-atmosphere flow W_{ca} . The latter causes a gross change in the pressure system, which then responds much differently to the input due to cushion flow W_{cu} .

Of course, the validity of the above analysis and discussion rests on the validity of the trunk geometry model used. Assuming the trunk model to be valid, the calculated stability behavior appears reasonable and explainable.

(4) Effect of frozen trunk model.

The previous results indicate that trunk shape sensitivity to trunk and cushion pressure variations is significant. For the cylindrical inelastic trunk model considered, the trunk moves in and out (also up and down) substantially during the plunge motion of the vehicle. For an actual single piece trunk, however, some restraint of this trunk motion will be provided by the trunk assembly curvature (in the horizontal plane), which is accompanied by a restraining tension in the horizontal plane. For example, in the limiting case of a toroidal or doughnut-shaped trunk, this horizontal tension would provide a significant restraining influence on trunk shape change. In fact, if the trunk material were truly inelastic, trunk outward movement (as occurs in the present model, for instance, when cushion pressure increases) would be difficult since such movement would have to be accompanied by stretching of the trunk. Thus, the trunk shape characteristics exhibited by a doughnut-shaped trunk might be expected to be more like those of the Boeing frozen trunk model than like those of the inelastic membrane model.

A preliminary assessment of the effect on stability of such trunk shape change restraint was made by calculating the stability characteristics using the frozen trunk geometry model developed by Boeing (Ref. 1). A second reason for making calculations for a different type of trunk model was to determine whether the previously noted destabilizing tendency of the cushion end flow W_{cu} /altitude sensitivity appears to be a general characteristic of air cushion landing systems or is peculiar to the particular inelastic membrane model considered.

The key feature of the frozen trunk model relative to the membrane model is that the trunk shape no longer depends on trunk and cushion pressures. Thus, in the variational stability equations given in Table 1, all partial derivatives with respect to P_c and P_t are deleted; the geometry parameters are calculated using the free shape model with pressure ratio $P_r = 0$. For this frozen trunk model, the sta-

bility behavior in the neighborhood of first ground contact was determined for system parameters and operating conditions closely approximating those used in the inelastic membrane model analysis: all system flows were chosen to be the same as those previously used at first ground contact. Then, the geometric parameter Y_a was increased to 4.76 in. in order to keep the equilibrium cushion volume V_c the same as before (and to prevent the two trunk elements from "passing through" each other). This resulted in an increase in equilibrium cushion pressure to $P_c = 16.063$ psi and in equilibrium altitude to $h = 4.193$ ft. with trunk pressure P_t unchanged. The cushion end flow W_{cu} /altitude sensitivity was then made to be the same as before, as were all other parameters.

For this system and operating point the partial derivatives with respect to altitude required to determine the stability matrix were calculated for the cases just before and just after ground contact. Since all partial derivatives with respect to cushion and trunk pressure are zero for the frozen trunk, the stability matrix was altered substantially when compared to the unrestrained model case. The resulting stability matrix is shown below for the case preceding ground contact; the two coefficients a_{24} and a_{34} shown in parentheses represent the only changes which occur following ground contact.

$$[A] = \begin{bmatrix} -30.8 & 17 & 0 & 0 \\ 101.2 & -226.2 & 46.6 & (-9576) \\ 0 & -23.6 & 0 & -24076 \\ 0 & 0 & -1 & (3041) \end{bmatrix}$$

Of note is that the pressure system portion of this matrix (upper left hand 2×2 submatrix) is the same before and after ground contact. The changes in $[A]$ are due to (1) cutoff of the cushion to atmosphere flow W_{ca} , which reduces the input a_{24} to the pressure system, and (2) the altitude dependence of the geometric parameters Y_o

and L_3 following ground contact (a_{34}), which stiffens the plunge mode motion. The four system eigenvalues resulting before and after ground contact are given below:

Before Contact

$$\begin{aligned}\lambda_1 &= -239.7 \\ \lambda_2 &= -28.8 \\ \lambda_{3,4} &= 5.76 \pm 50.3i\end{aligned}$$

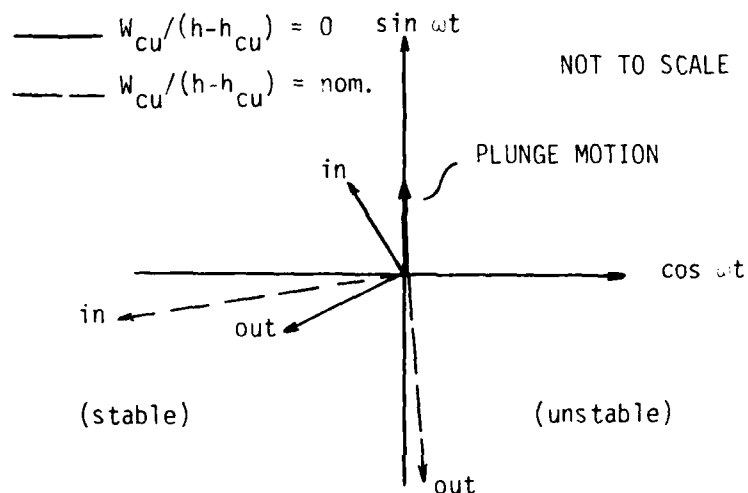
After Contact

$$\begin{aligned}\lambda_1 &= -234.1 \\ \lambda_2 &= -24.2 \\ \lambda_{3,4} &= .65 \pm 63.6i\end{aligned}$$

These results show predicted behavior which is much different than that calculated for the inelastic trunk model. In this case instability is predicted both before and after ground contact. Moreover, the plunge motion is predicted to be less unstable following ground contact, which is opposite the trend occurring for the inelastic model. In assessing the cause of this behavior, we first note that the pressure system eigenvalues λ_1 and λ_2 are close to those obtained for the inelastic model prior to ground contact (Table 2). Thus, the "mechanical oscillator" used to represent the pressure system is roughly the same as for that case (for which the plunge motion was stable). However, the oscillator used to represent the vehicle plunge motion is now much stiffer due to restraint of trunk shape change. This results in a near resonant condition in the pressure system when a harmonic plunge motion is input. Furthermore, the magnitude of input to the pressure system is much larger for the frozen model, e.g. compare magnitudes of a_{24} for the frozen and unrestrained trunks. It, therefore, appears that the predicted unstable behavior of the frozen trunk results primarily from the substantial stiffening caused by trunk restraint. This is distinctly different than the unstable behavior of the unrestrained model following ground contact, which is due mainly to changes in the pressure system behavior.

In order to assess the influence on stability of the cushion end flow $W_{cu}/\text{altitude sensitivity}$, plunge mode eigenvalues were calculated for the frozen trunk model following ground contact with $W_{cu}/(h-h_{cu}) = 0$, which represents direct cushion to

atmosphere throttling. In this case, the plunge mode eigenvalues were $\lambda_{3,4} = -2.3 \pm 56i$. This shows that the end cushion to atmosphere flow sensitivity to altitude is destabilizing, the same trend exhibited by the unrestrained model. The reason for this tendency for the frozen trunk is that, although the pressure system is still operating in a near resonant condition, the input to the system has been shifted substantially and is much weaker. The phasing relations following ground contact are shown below for both the nominal $W_{cu}/(h-h_{cu})$ and for $W_{cu}/(h-h_{cu}) = 0$:



Calculations similar to the above for the case just prior to ground contact and with no cushion end flow/altitude sensitivity yielded plunge mode eigenvalues of $\lambda_{3,4} = 2.6 \pm 40i$. This represents a noticeable reduction in the degree of instability and, although physically unrealistic, does indicate the degree to which the stability is influenced by the end cushion to atmosphere flow.

Thus, the implication of these results is that the plunge mode stability will be improved if the altitude sensitivity of cushion end flow can be minimized or eliminated.

SECTION III

MODEL VALIDITY ASSESSMENT

1. Model Limit Cycle Behavior

All preceding discussion applies to infinitesimal motion as governed by the linearized versions of equations (1) - (4). In order to verify these results and to assess the influence of system nonlinearities on the response, equations (1)-(4) were integrated numerically for several operating conditions. It was anticipated that limit cycles would occur for operation near an unstable equilibrium condition. An important objective of the numerical work was to determine whether the amplitude of such limit cycles would follow the same trends as those outlined in Section II.3.6, "Parameter Change Effects on Stability." For example, consider operation at a trunk flow rate W_{tr} slightly greater than that associated with first ground contact, for which the original model was highly unstable. Now, by decreasing the cushion end flow W_{cu} altitude sensitivity, the linear stability is improved (Figure 7), and it might be expected that the associated limit cycle would be less violent than that occurring for the original system. This behavior was checked by simulating the motion at a trunk flow rate $W_{tr} = 770$ lb/min for both the original end cushion flow/altitude sensitivity $W_{cu}/(h-h_{cu}) \cong 200$ lb/ft-sec and for $W_{cu}/(h-h_{cu})$ reduced by a factor of five. These results are shown in Figures 8 and 9, in which are plotted the histories of altitude h , trunk pressure P_t , and cushion pressure P_c for these two cases. In each case a limit cycle is approached in the first three seconds of the simulation. The factor of five reduction in $W_{cu}/(h-h_{cu})$ results in a vehicle motion h amplitude of about 40% that occurring for the original system. Even larger reductions are noted in the pressure amplitudes. Thus, qualitatively, both linear stability and nonlinear behavior are improved by the reduction in cushion end flow/altitude sensitivity.

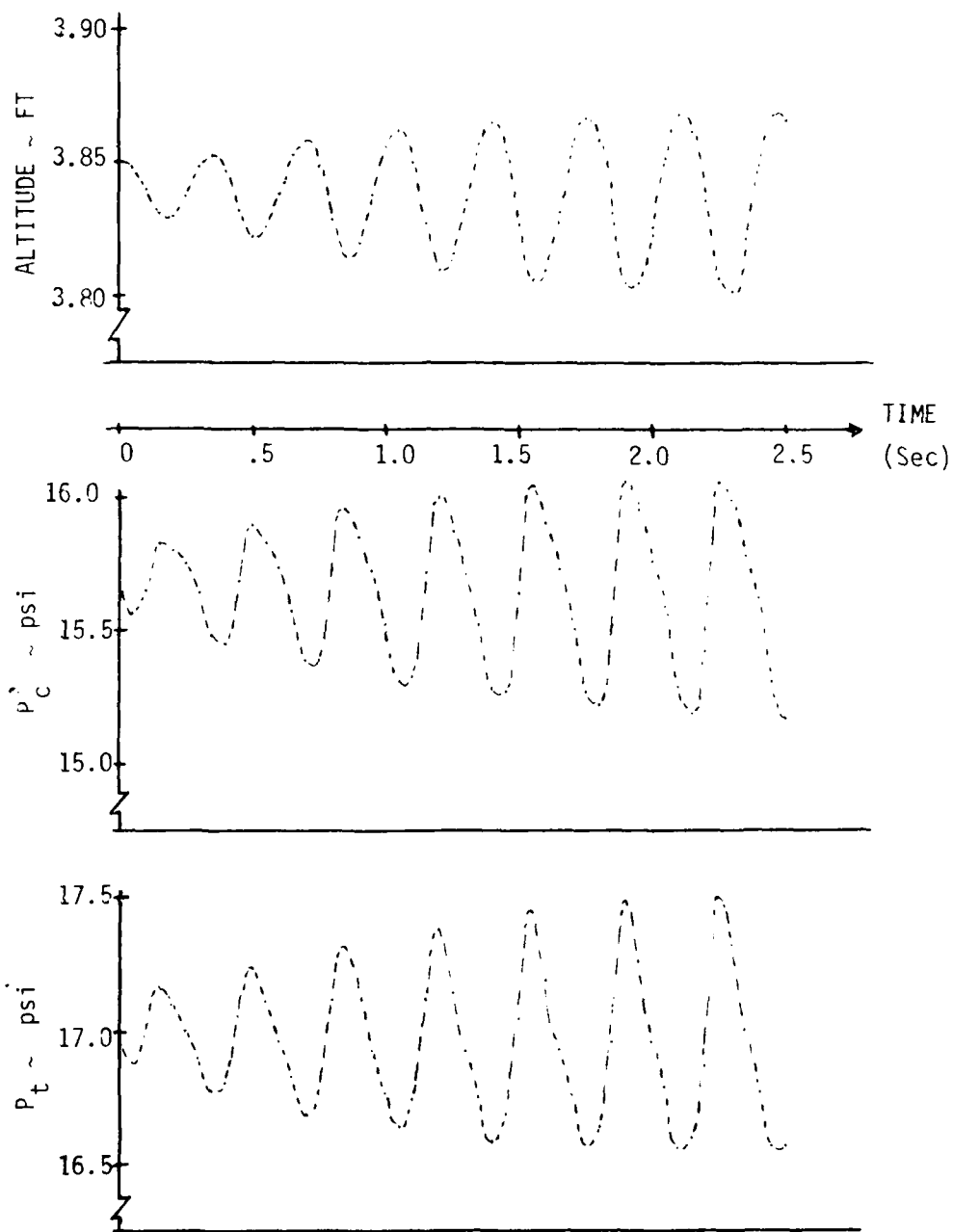


Figure 8 - Limit Cycle Behavior: $W_{tr} = 770 \text{ lb/min}$, Nominal $W_{cu}/(h-h_{cu})$

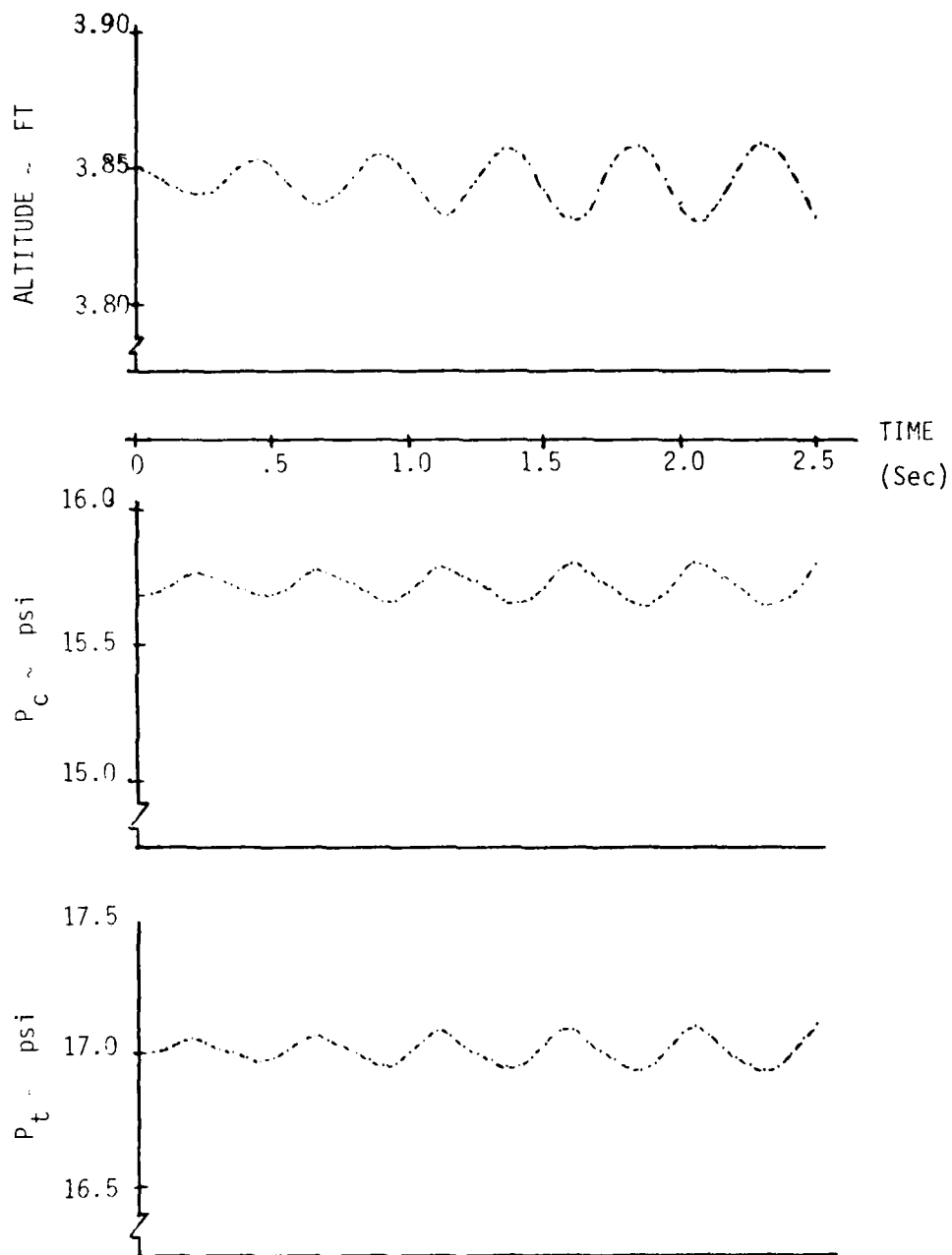


Figure 9 - Limit Cycle Behavior: $W_{tr} = 770$ lb/min, $V_{cu}/(h-h_{cu}) = .2$ of Nominal

There are several features exhibited in Figures 8 and 9 which are consistent with the linearized results. For instance, the frequency of limit cycle motion is essentially the same as that given by the plunge mode eigenvalue: for the nominal case $W_{cu}/(h-h_{cu}) \cong 200$ lb/ft-sec the limit cycle frequency obtained from the simulation is approximately 17.8/sec, while for $W_{cu}/(h-h_{cu})$ reduced by a factor of five, the limit cycle frequency is approximately 13/sec. These values are in good agreement with the linearized results shown in Figure 7 for $W_{tr} = 757$ lb/min. The implication is that system stiffness properties remain essentially linear during large amplitude motion.

A second feature of the limit cycle behavior which is similar to that predicted by the linear analysis is that the cushion and trunk pressure amplitudes and phasings are about the same. The describing function results given by equations (20) and (21) exhibit this behavior for most of the cases considered in this study. In addition to this feature, the reduction in the ratio of pressure to altitude amplitudes which occurs when $W_{cu}/(h-h_{cu})$ is reduced is consistent with the describing function interpretation that a reduction in $W_{cu}/(h-h_{cu})$ results in a reduction in input to (and hence output from) the pressure system.

Additional simulation results are shown in Figures 10 and 11 for a trunk flow rate $W_{tr} = 840$ lb/min. Figure 10 represents the nominal system, while the results shown in Figure 11 represent a factor of four reduction in $W_{cu}/(h-h_{cu})$. In the latter case the limit cycle amplitude is about half that predicted for the nominal system. The qualitative features of the motion and pressure response at this flow rate are consistent with the linear results, as in the case $W_{tr} = 770$ lb/min.

The behavior at this trunk flow is more violent than at the lower flow rate of 770 lb/min. The reason for this appears to be the influence of altitude on system damping. Presumably, energy is fed to the motion when the altitude is near its unstable equilibrium value and dissipated at altitudes away from equilibrium,

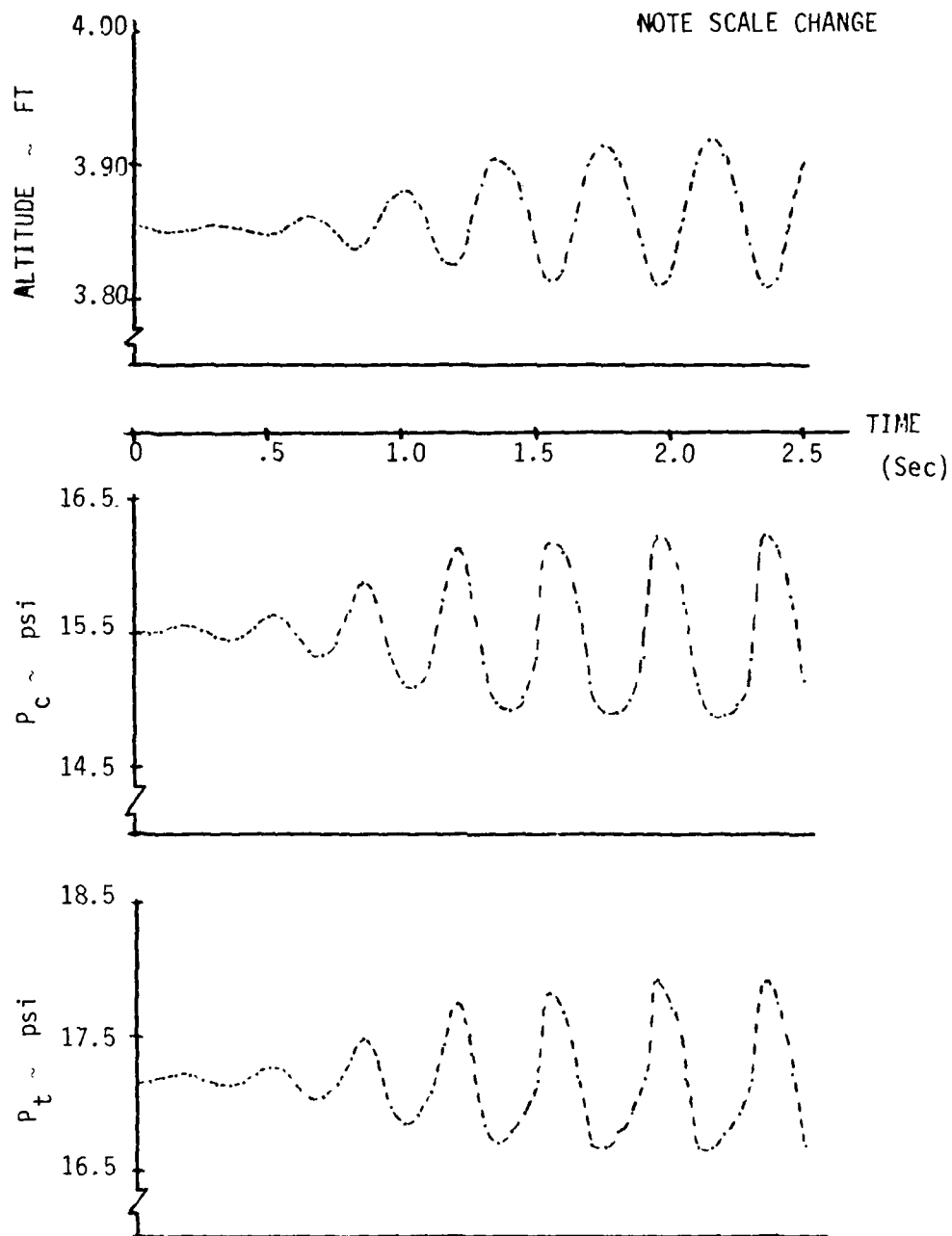


Figure 10 - Limit Cycle Behavior: $W_{tr} = 840 \text{ lb/min}$, Nominal $W_{cu}/(h-h_{cu})$

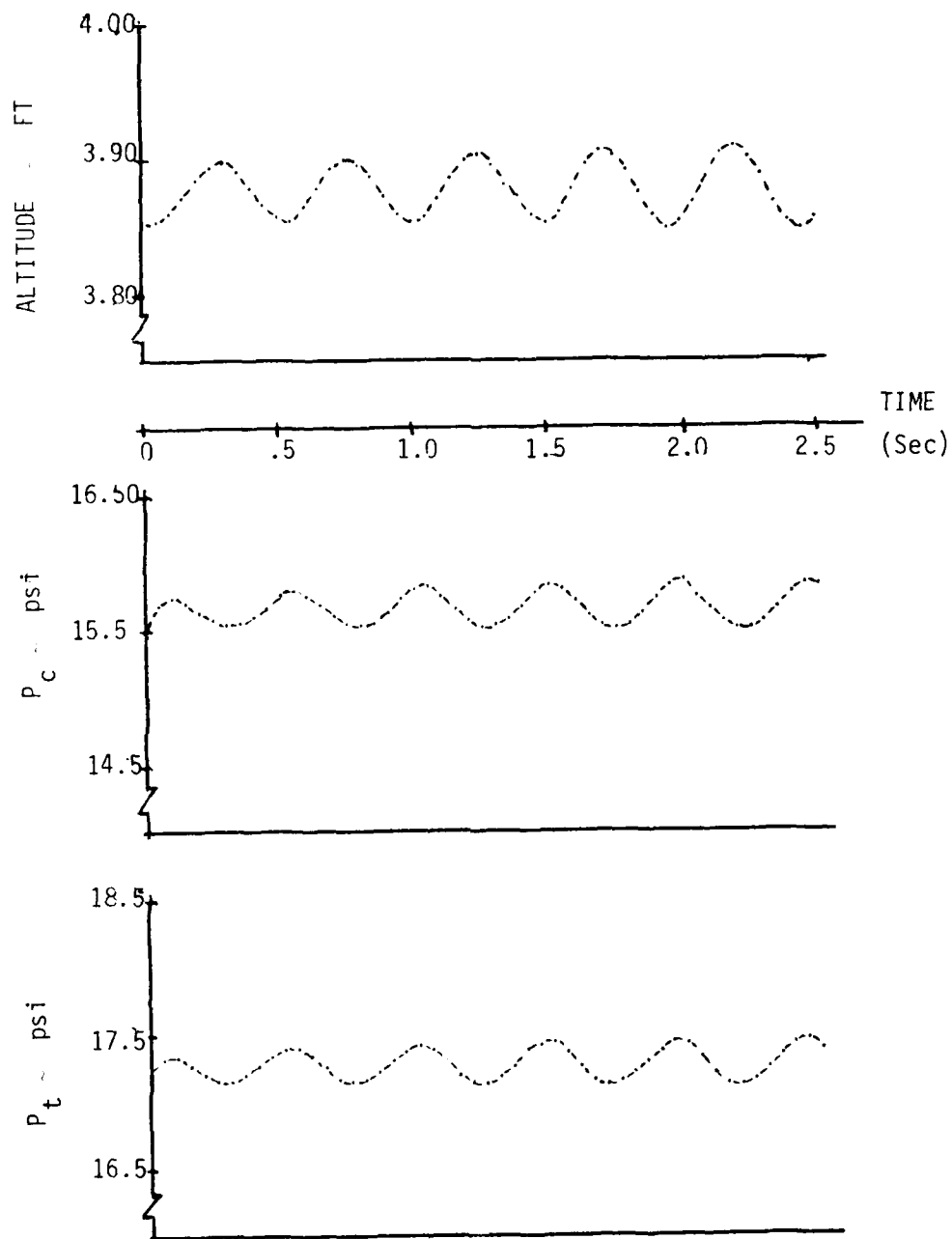


Figure 11 - Limit Cycle Behavior: $W_{tr} = 840$ lb/min, $W_{cu}/(h-h_{cu}) = .25$ of Nominal

so that on the average the energy change per cycle is zero. It appears that when the equilibrium conditions are close to a stability boundary (e.g., at 770 lb/min), less altitude oscillation is needed to provide a cycle by cycle energy balance than when equilibrium is not near a stability boundary (e.g., at 840 lb/min).

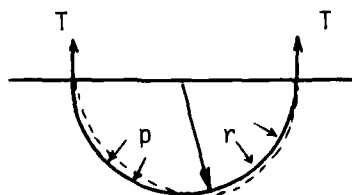
A simulation was also made for trunk flow $W_{tr} = 950$ lb/min and in this case a slight deviation from equilibrium was damped out, in agreement with the linear stability results. We note that a limit cycle could probably be induced in this case even though equilibrium is stable. For initial conditions which deviate substantially from equilibrium a large amplitude limit cycle may be possible. From a practical standpoint, however, limit cycles would be most likely to occur for unstable equilibrium conditions.

2. Trunk Model

Several aspects of the trunk model were assessed, since the dynamic behavior is sensitive to the dependence of trunk geometry on pressure and altitude.

a. Trunk Inertia

The trunk geometry model was developed based on a static force balance (Reference 1). As the vehicle undergoes plunge motion, the trunk moves in and out in response to the pressure variations which accompany the motion. Thus, if trunk inertia is appreciable the trunk geometry existing during the motion will differ from that predicted statically. The importance of this effect was assessed by calculating the approximate frequency of a semi-circular trunk element under internal pressure as shown schematically below (the lowest mode displaced shape for an inelastic trunk is also shown):



Using mass and geometric properties of the Jindivik trunk (density of 1 lb/yd²) and the approximate frequency relation $\omega = (T/\rho)^{1/2}/r$, the natural frequency should be in excess of 200-250 rad/sec. Since the plunge mode frequency is substantially less than this, the trunk response will be essentially static, and trunk inertia effects on vehicle response will be slight. This is especially true for the unrestrained trunk, whose frequency is $\omega < 20$ rad/sec. Even for a trunk which is restrained and therefore exhibits a higher plunge frequency (e.g., the frozen model where $\delta \sim 50-60$ rad/sec), the importance of inertia effects should still be slight for the vehicle/cushion system considered here.

If the plunge mode and trunk natural frequencies were comparable, the resulting trunk shape response would lag that calculated statically, and this in turn would cause a change in the pressure system response, particularly the phasing of the pressure system output. Rigorous modeling of the associated effect on vehicle stability would be difficult, because the lowest trunk mode damping would have to be determined; practically, this could be best estimated through testing.

b. Trunk Curvature

The model analyzed in this study consisted of four trunk elements which were physically isolated from each other: the two unrestrained side elements and the frozen end elements (isolated elements are also a characteristic of the general trunk model described in Reference 1.) This type of model should work reasonably well if the side elements are long relative to the end ones. Nevertheless, for a single piece trunk the curvature (in horizontal plane) at the "corners" will provide some restraint due to the tensile forces developed in the horizontal plane. Whether or not this would tend to destabilize the vehicle would depend primarily on the relative changes in plunge frequency and pressure system response, as discussed previously in comparing the unrestrained and frozen models. Since for the

system analyzed the stability appears better if the side and end elements are truly isolated, the possibility of designing a trunk to exhibit this behavior should be considered.

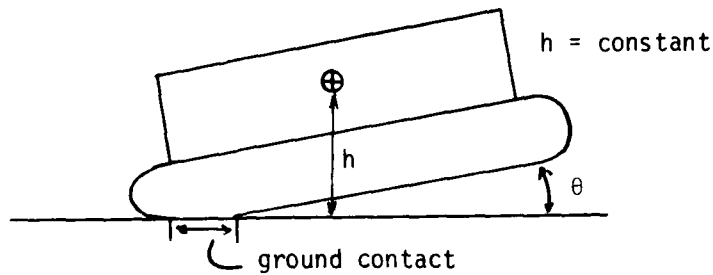
c. Other Effects

Several effects not included in the present model may be of importance and are noted here. First, the flow areas for trunk to cushion and trunk to atmosphere flows will change as the trunk comes into ground contact and a portion of the perforations are blocked. In the model studied here these flow areas were assumed constant. Changes in these flow areas with altitude will alter the manner in which the operating point (h, P_c, P_t) varies with trunk flow W_{tr} after ground contact. However, the destabilizing tendency occurring at first ground contact in the present model should also appear with a variable flow area model, since the blocked area at first trunk-ground contact would be very small.

A second effect not included in the present model was the interaction of trunk pressure and fan performance. Such interaction has been noted experimentally by Leland, et al (Reference 3). A result of such interaction would be a variable trunk flow, $W_{tr} = W_{tr}(P_t)$. This would alter the pressure system portion of the variation equations given in Table 1. Qualitatively the result would be a quicker pressure response; a slight increase δP_t would cause a small decrease δW_{tr} , which in turn would contribute to a negative $\delta \dot{P}_t$. Thus, for the model analyzed the stability would be expected to improve slightly.

3. Effect of Pitch Motion

In the present study no attempt was made to include vehicle motions other than vertical translation. The intent of the present section is to point out that vehicle pitch will result in coupled motion/pressure characteristics which differ from those exhibited in the plunge mode. For example, consider a vehicle undergoing pitch motion with the c.g. fixed, as sketched below.



The flow area between trunk and ground (which passes W_{ca}) will be constant during the pitching motion provided that no trunk/ground contact occurs. In this case the air flows will have no sensitivity to the motion, and small pitch deflections about equilibrium would be neutrally stable, since there is no "spring" in the system.

On the other hand, if ground contact were to occur over a portion of the trunk during the motion, then the cushion to atmosphere flow would be decreased, resulting in a motion induced input to the pressure system. Furthermore, this area decrease would occur twice during a single cycle of pitch, so that the motion induced input to the pressure system would be at a frequency which is twice the pitch frequency. The pressure response would also be at twice the pitch frequency. A limit cycle would be expected to occur, since the trunk/ground contact moment would restrain the motion. This type of behavior has been observed by Leland, et al (Reference 3) in their testing of a $\frac{1}{4}$ scale model of the CC-115 aircraft. Analytical study of this phenomenon would be complicated by the fact that the trunk/ground contact properties would be nonuniform along the trunk section.

SECTION IV

CONCLUSIONS

The vehicle/ACLS model studied is stable for operation with no trunk-ground contact and unstable for a range of operating conditions for which no trunk-ground contact occurs. The destabilizing influence of first trunk-ground contact is due, on the one hand, to the cut-off of air flow beneath the side elements and, on the other, to the strong altitude sensitivity of the remaining flow beneath the frozen end elements. These effects combine to cause a substantial change in the trunk and cushion pressure responses and hence in the vertical forces on the vehicle. The effect is configuration dependent and sensitive to the trunk geometry variation with pressure and altitude.

For this model the instability could be eliminated by ensuring that ground contact of both side and end elements occurs simultaneously, and by also venting the cushion directly to the atmosphere through a constant area orifice. The destabilizing effect predicted for the original model is physically reasonable and is similar to the classical self-excited vibration phenomenon, with the power required to drive the input flow W_{tr} as the source of energy.

The analytical approach used to study the stability behavior appears to provide a useful tool for design of systems of this type so that acceptable stability behavior is achieved.

SECTION V

RECOMMENDATIONS

For the inelastic model considered, the trunk and cushion pressures significantly influence the trunk shape and hence the nature of forces acting on the vehicle. For an actual trunk, and especially for one which may be unlike the present model, measurement of these trunk shape characteristics would be useful in assessing the validity of the trunk model used. For instance, static experimental determination of the dependence of Z_0 , Y_0 , and L_3 on pressure ratio $(P_c - P_a)/(P_t - P_a)$ for cases with and without ground contact would enable the validity of a trunk shape model to be assessed. Measurement of the free vibrational characteristics of the lowest mode of trunk oscillation would also enable the importance of trunk inertia to be determined.

The possibility of improving stability behavior through feedback control may be of interest. For instance, if the cushion were vented directly to atmosphere, a variable orifice area could be used to vary the cushion to atmosphere flow so as to augment stability (this possibility is suggested because of its relative simplicity).

REFERENCES

1. Wahi, M.K., Duleba, G.S., Kilner, J.R., and Perkins, P.R., "EASY - ACLS Dynamic Analysis, Vol. I - Computer Mathematical Models," AFFDL-TR-79-3105, September 1978.
2. Burton, T.D., "ACLS Model Stability Study," February 1980.
3. Leland, T.J.W., Thompson, W.C., and Vohinger, D.S., "Preliminary Results from Dynamic Model Tests of an Air Cushion Landing System," in Air Cushion Landing Systems, ed. H. Saha, Miami Beach, FL, December 12-14, 1972.